ESTRUCTURA GALÁCTICA
Y
DINÁMICA ESTELAR

Cúmulos de Estrellas

Cúmulos de Estrellas

propiedades

Cúmulos de Estrellas: abiertos × globulares

	CAb	CGl
Riqueza	$10\text{-}10^3$	$10^3\text{-}10^6$
Forma	irregular	~ esférica (b/a ~ 0.93)
Diámetro	4-12 pc	25-100 pc
Masa	$10^2\text{-}10^5\ M_\odot$	$10^4\text{-}10^7\ M_\odot$
Luminosidad	–3 … –9	–3 … –10.4 (ωCen)
Población	I	II
ISM	si (formación estelar)	no
Metalicidad	$-0.75 \leq [Fe/H] \leq 0.4$	$-2.5 \leq [Fe/H] \leq -1.0$ (halo) $-1.0 \leq [Fe/H] \leq 0.0$ (disco)
Edad	jóvenes (10^8 a) intermed. (1-10 Ga)	viejos (8-14 Ga)
Dinámica interna	inestables (?)	estables (ligados + equilibrio)
n	$100\ M_\odot\ pc^{-3}$	$8000\ M_\odot\ pc^{-3}$
(r_c, r_h, r_t) [cuartiles]	(1-2, 2, 10-20) pc	(0.5-2.5, 2-5, 20-60) pc
Distribución (VL)	disco (brazos espirales)	halo, disco grueso
Cantidad (VL)	1690 (10^5 ?)	160 (200 ?)
Otras galaxias	Sp, Irr (dE del GrL)	todos los tipos

Table 6.2 Characteristics of selected open clusters

Name NGC	Name Other	D (kpc)	$(R,z)_{\rm gal}$ (kpc)	M_V	Diameter (arcmin)	Trumpler class	$(B-V)_{\rm TO}$	$\log(t/{\rm yr})$	[Fe/H]	Comments
2264	–	0.79	(9.23,0.03)	−5.4	40	III,3,p,n	−0.25	6.5 – 7.0	−0.15	Typical young cluster
6705	M11	1.72	(6.96,−0.08)	−5.4	13	I,2,r,-	−0.05	8.4	+0.05	Typical intermediate-age cluster
188	–	1.55	(9.35,0.58)	−2.9	15	II,2,r,-	+0.58	9.8	−0.16	Typical old cluster
6791	–	4.20	(8.12,0.80)	−3.6	10	I,2,r,-	+0.60	10.0	+0.15	Very old metal-rich cluster
7261	–	2.12	(9.23,0.03)	−3.2	6	III,1,p,-	−0.25	7.6	−0.46	Young metal-poor cluster
–	Berkeley 17	2.40	(10.89,−0.15)	–	8	III,1,r,-	+0.58	10.1	−0.29	Oldest known cluster
–	Berkeley 20	8.14	(16.12,−2.42)	–	3	I,3,p,-	–	9.7	−0.75	Metal-poorest known cluster
–	Hyades	0.05	(8.55,−0.02)	−2.5	329	II,3,m,-	+0.12	8.8	+0.19	Nearby cluster, classically used to establish the distance scale
–	Coma, Mel 111	0.08	(8.56,0.07)	−2.9	275	III,3,p,-	+0.05	8.6	−0.03	Nearby poor cluster
–	Pleiades, M45	0.13	(8.63,−0.05)	−3.7	109	I,3,r,n	−0.11	8.0	+0.11	Nearby well-studied cluster
2632	Praesepe, M44	0.16	(8.64,0.08)	−2.9	95	II,3,m,-	+0.15	8.8	+0.19	Nearby well-studied cluster
869	h Persei	2.23	(10.19,−0.14)	−7.4	29	I,3,r,-	−0.25	6.7	−0.05	Rich young cluster, twin with χ Persei
884	χ Persei	2.22	(10.18,−0.14)	−7.3	29	I,3,r,-	−0.25	6.7	−0.05	Rich young cluster, twin with h Persei

NOTES: D is the distance to the cluster; $(R,z)_{\rm gal}$ are its cylindrical coordinates relative to the Galactic center; $(B-V)_{\rm TO}$ is the color of its main sequence turn-off point; t is its estimated age; other quantities are as defined in the chapter.

SOURCE: From the data collected in Lynga (1987), Meynet, Mermilliod & Maeder (1993) and Friel (1995).

Table 6.1 Characteristics of selected globular clusters

Name NGC	Name Other	$R_{\rm gal}$ (kpc)	M_V	r_h (arcmin)	log (r_t/r_c)	Spec. type	[Fe/H]	HB$_{\rm col}$	Comments
104	47 Tuc	7.3	−9.26	2.79	2.04	G4	−0.76	−0.99	Typical metal-rich cluster
5272	M3	11.6	−8.77	1.12	1.85	F6	−1.57	+0.08	Typical intermediate-metallicity cluster
7078	M15	10.2	−9.07	1.06	2.50	F3	−2.22	+0.67	Typical metal-poor cluster. Collapsed core
288		11.4	−6.54	2.22	0.96	F8	−1.24	+0.98	Same [Fe/H] as NGC 362, but has a blue HB
362		9.0	−8.26	0.81	1.94	F9	−1.16	−0.87	Same [Fe/H] as NGC 288, but has a red HB
1851		16.3	−8.26	0.52	2.24	F7	−1.26	−0.36	Same [Fe/H] as NGC 288,362, but bimodal HB
5139	ω Cen	6.3	−10.16	4.18	1.24	F5	$-2\ldots-1$	+0.90	Most luminous. Chemically inhomogeneous
	AM 4	24.2	−1.50	0.42	0.50		−2.00	+0.98	Least luminous. Least concentrated core
6121	M4	6.1	−7.06	3.65	1.59	F8	−1.18	−0.06	Closest cluster ($d = 2.1\,{\rm kpc}$)
	AM 1, E 1	117.2	−4.60	0.50	1.23		−1.80	−0.93	Most distant cluster
	Liller 1	2.3	−7.42	0.45	2.30		+0.22	−1.00	Most metal-rich. Collapsed core
5053		16.5	−6.64	3.50	0.82		−2.41	+0.52	Most metal-poor

NOTES: $R_{\rm gal}$ is the radius in the Galaxy at which the cluster lies; r_h is the half-light radius; other quantities are as defined in the text.

SOURCE: From data collected in Harris (1996).

Harris (1996), AJ 112, 1487

Definición y Clasificación

- Cúmulos Abiertos (clasificación de Trumpler):
  - → grado de concentración: **I** (más concentrado) … **IV** (menos concentrado)
  - → brillo: **1** (menor rango de brillos de estrellas) … **3** (mayor rango)
  - → riqueza: **p** (< 50), **m** (50-100), **r** (>100)
  - → ISM: **n** (nebulosa emisión/difusa asociada a las estrellas)

Trumpler (1930), Lick Obs. Bul. 14, 154

- Asociaciones (OB o T):
  - → muy baja densidad
  - → pequeño realce en la cantidad de estrellas

- Cúmulos Globulares (criterios):
  - → aprox. circulares (presumiblemente esféricos)
  - → sistemas puramente estelares (sin ISM)
  - → clases de concentración: **I** (mayor grado de conc. central) … **XII**

Shapley & Sawyer (1927), Harvard Obs. Bul. 849, 1

Observación

- Ventajas:
  - → las estrellas-miembros están a aprox. la misma distancia de nosotros
  - → tienen la misma edad y aprox. la misma metalicidad
  - → muchos CGl están fuera del plan de la Galaxia (poca extinción)
  - → la mayoría de los CAb son cercanos de nosotros (paralajes trigonométricas)
  - → hay muchos CAb (buena estadística)

- Problemas:
  - → extinción interestelar critica para los CAb
  - → confusión (superposición de estrellas, contam. en Lum.)
    especialmente para el centro de CGl
  - → contaminación con estrellas de campo, especialmente para CAb

CMD

Diagrama Color Magnitud

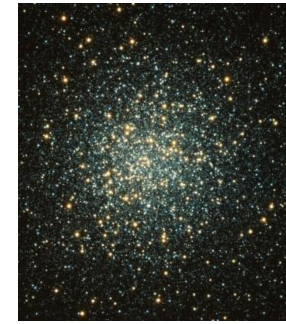

CAb

CGl

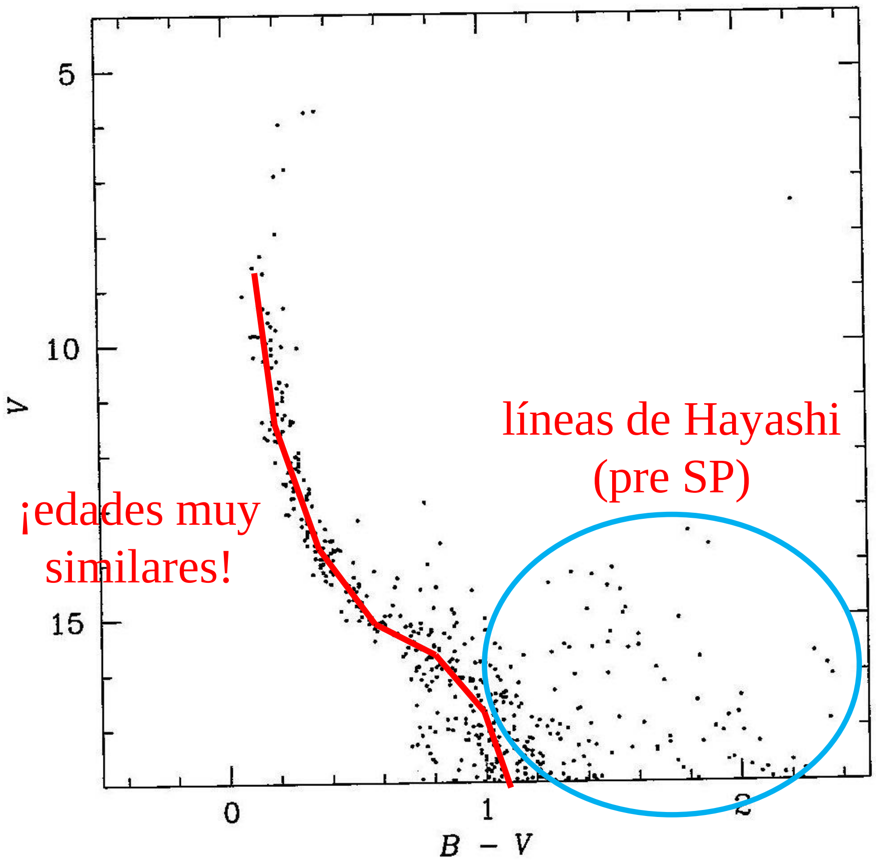

Figure 6.27 CM diagram of the young open cluster NGC 4755. Note the extensive MS, the scattering of stars to its right at faint magnitudes, and the single evolved supergiant star at the top right of the diagram. [From data published in Sagar & Cannon (1995) and Dachs & Kaiser (1984)]

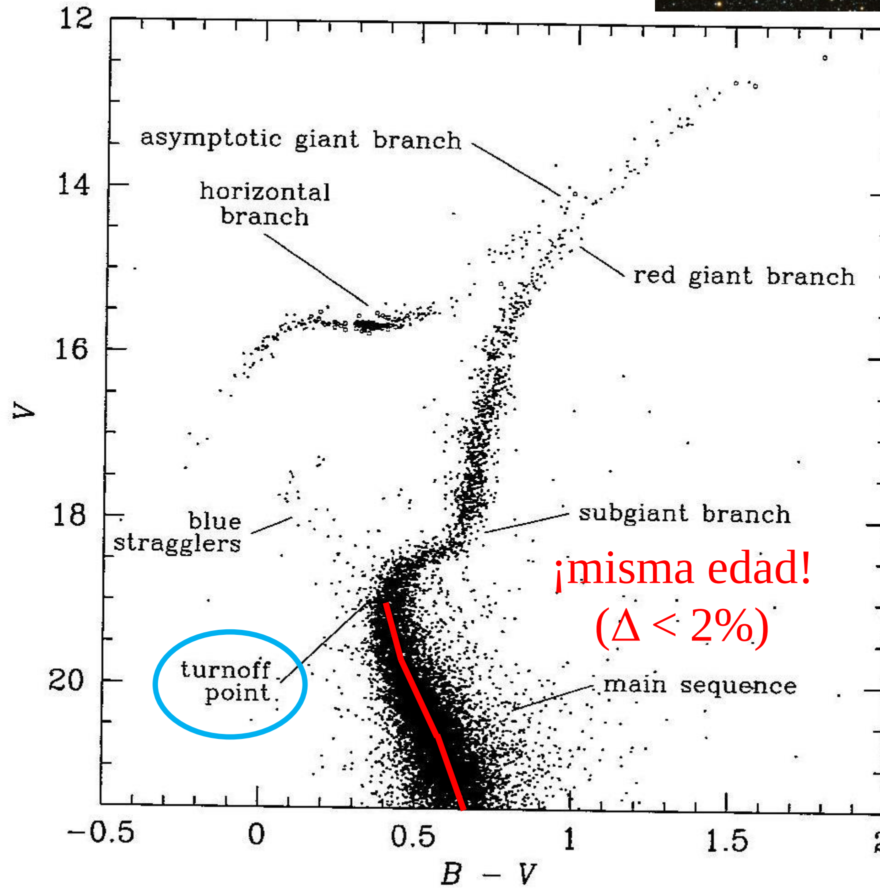

Figure 6.2 The color-magnitude diagram for the globular cluster M3. Known variable stars are shown as open circles, and the principal sequences are annotated. [From data published in Buonanno *et al.* (1994)]

CAb

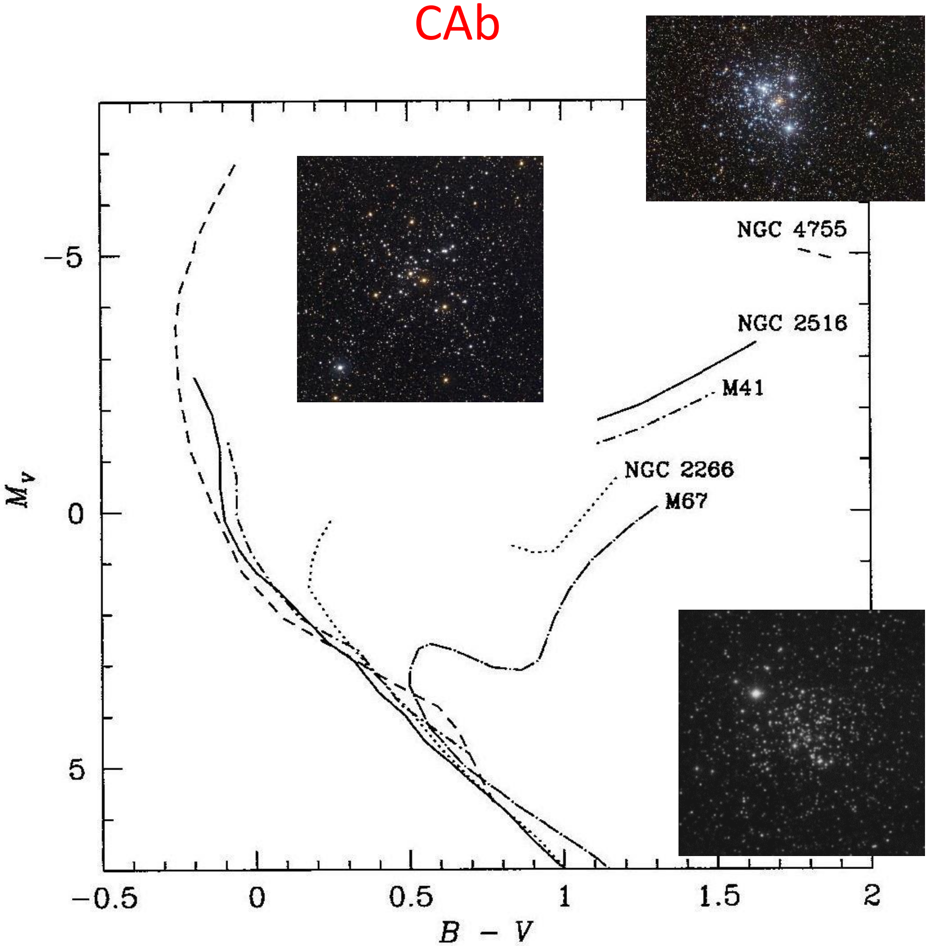

Figure 6.28 Sequences found in the CM diagrams of a number of open clusters, shifted to a common absolute-magnitude scale. [From data kindly provided by J.-C. Mermilliod]

CGl

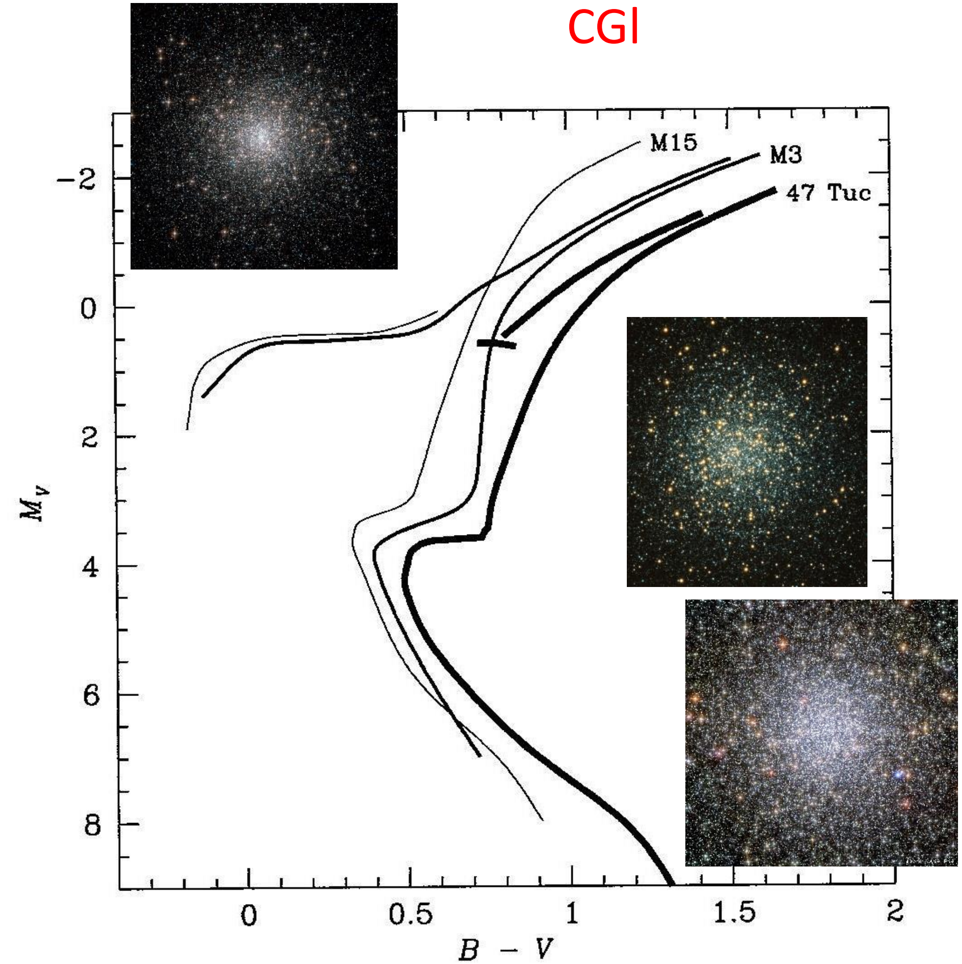

Figure 6.3 Schematic illustration of the principal sequences in the CM diagrams for three globular clusters. The systems shown are a metal-rich cluster (47 Tuc), an intermediate-metallicity cluster (M3), and a metal-poor cluster (M15). [Sequences from Hesser *et al.* (1987) and Buonanno *et al.* (1994)]

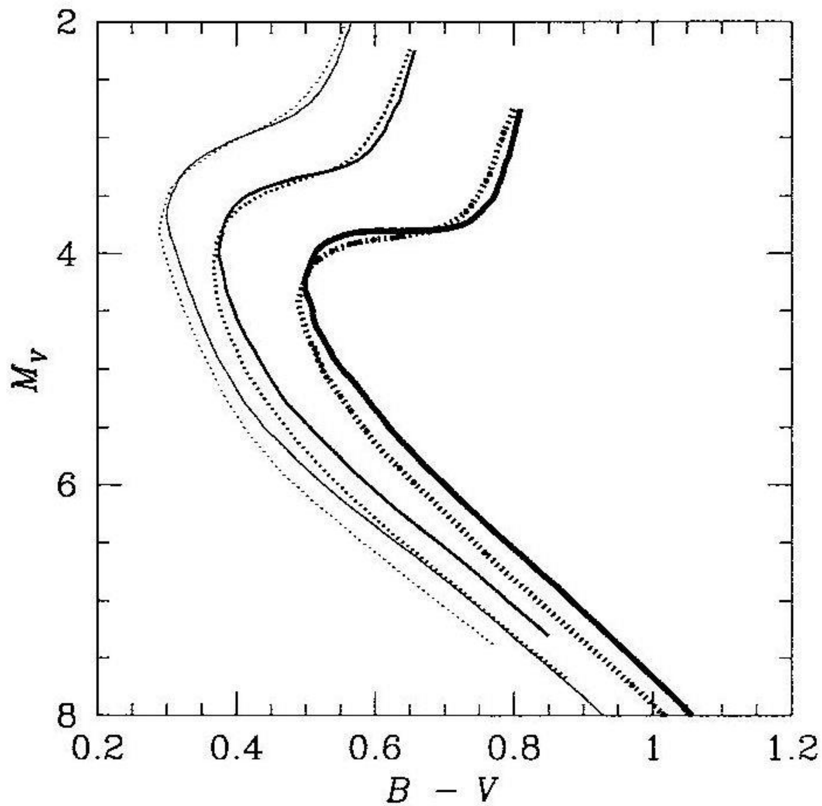

Figure 6.7 Illustration of the effects of varying Y and Z on the shape and position predicted for the 14 Gyr isochrone. The line width indicates the metallicity of the isochrone: the heaviest lines are for $Z = 0.006$; the intermediate lines are for $Z = 0.001$; and the lightest lines are for $Z = 0.0001$. The solid lines are for a Helium abundance of $Y = 0.2$, and the dotted lines are for $Y = 0.3$. [From the calculations of vandenBerg & Bell (1985)]

CAb

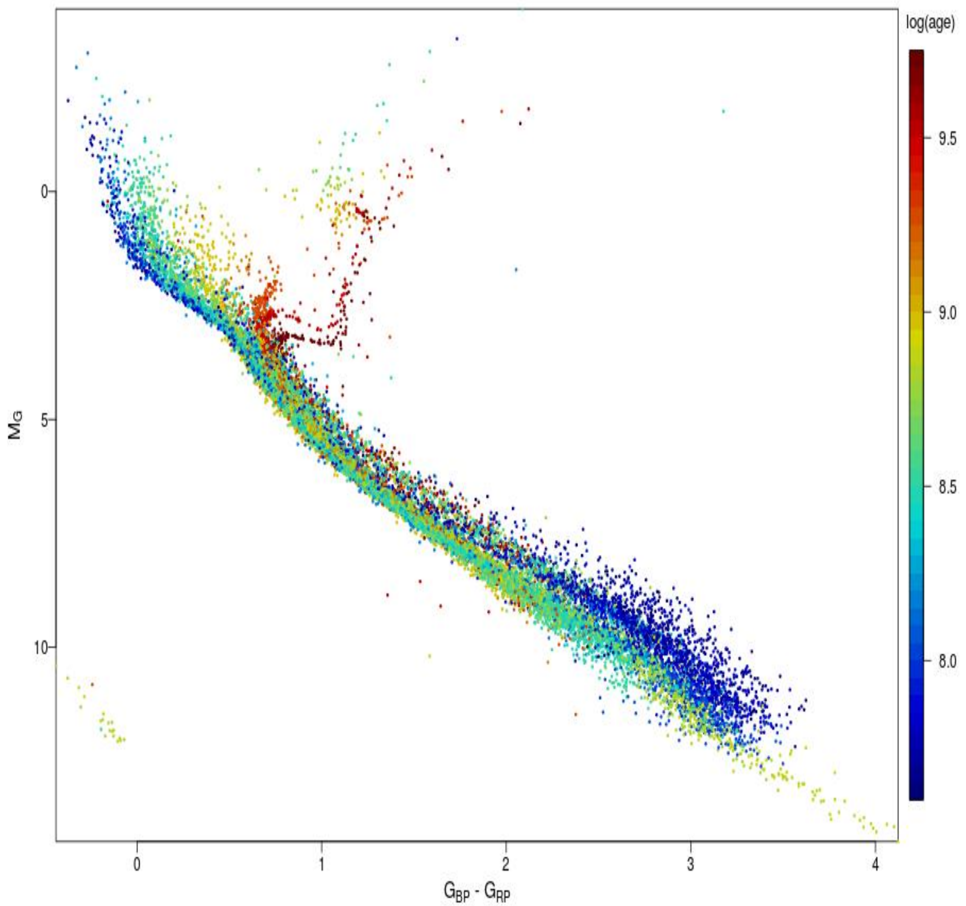

CGl

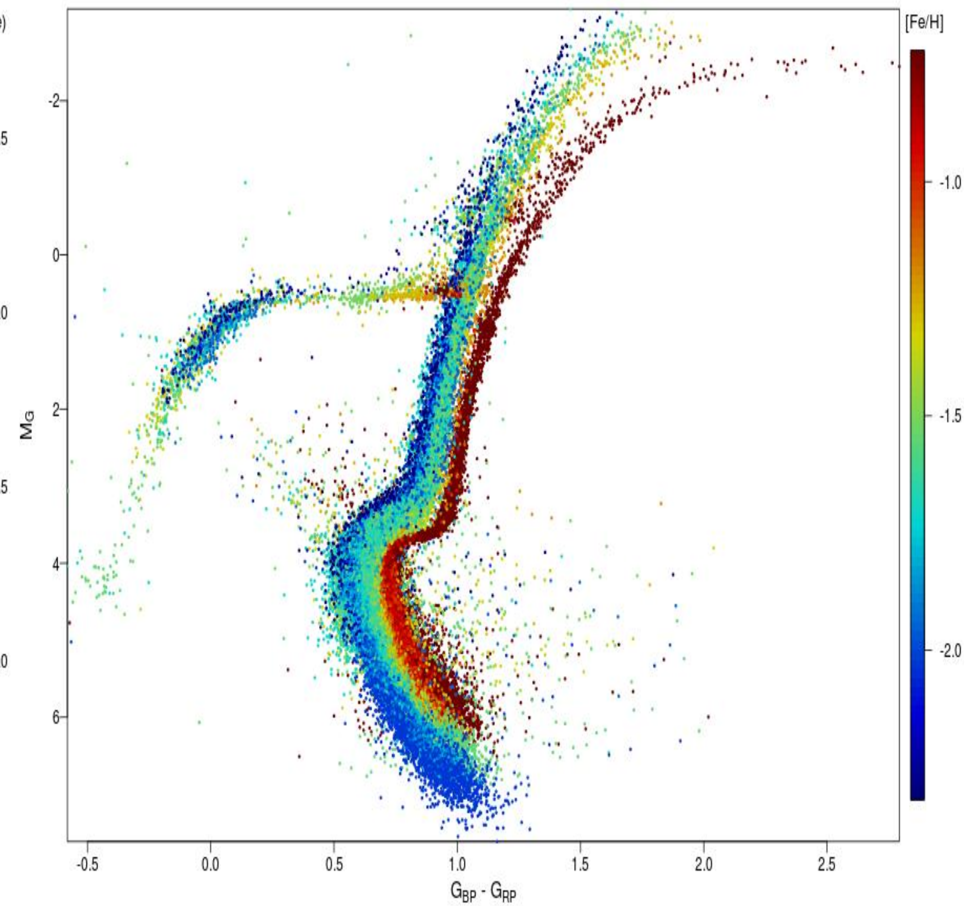

GAIA – *Data Release* 2 (2018)

CAb: 32 cúmulos abiertos, separados de los más jóvenes a los mas viejos.

CGl: 14 cúmulos globulares, separados de los mas pobres a los mas ricos en metales.

Rama Horizontal (HB)

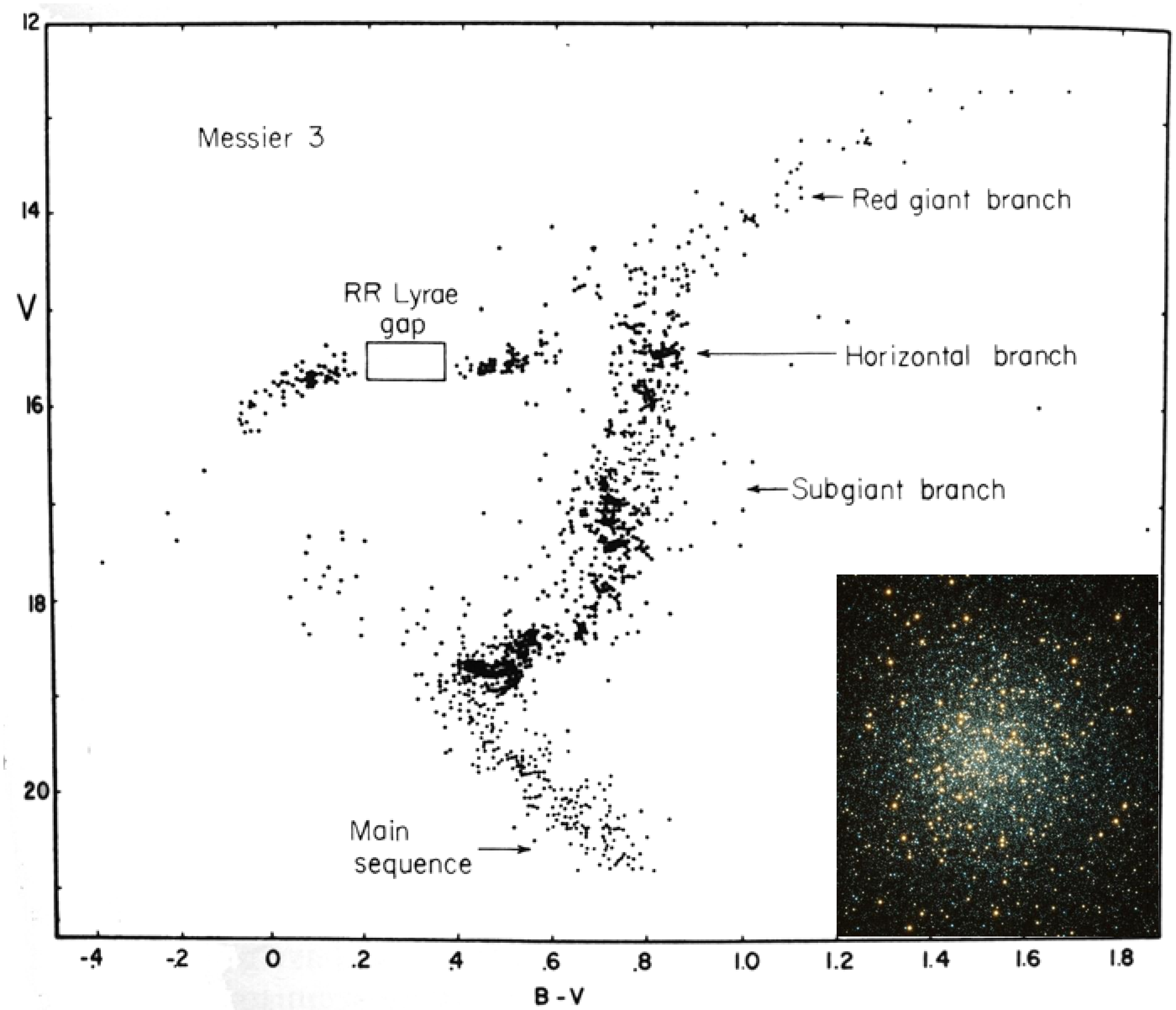

M15 - Globular Cluster with RR-Lyrae Stars

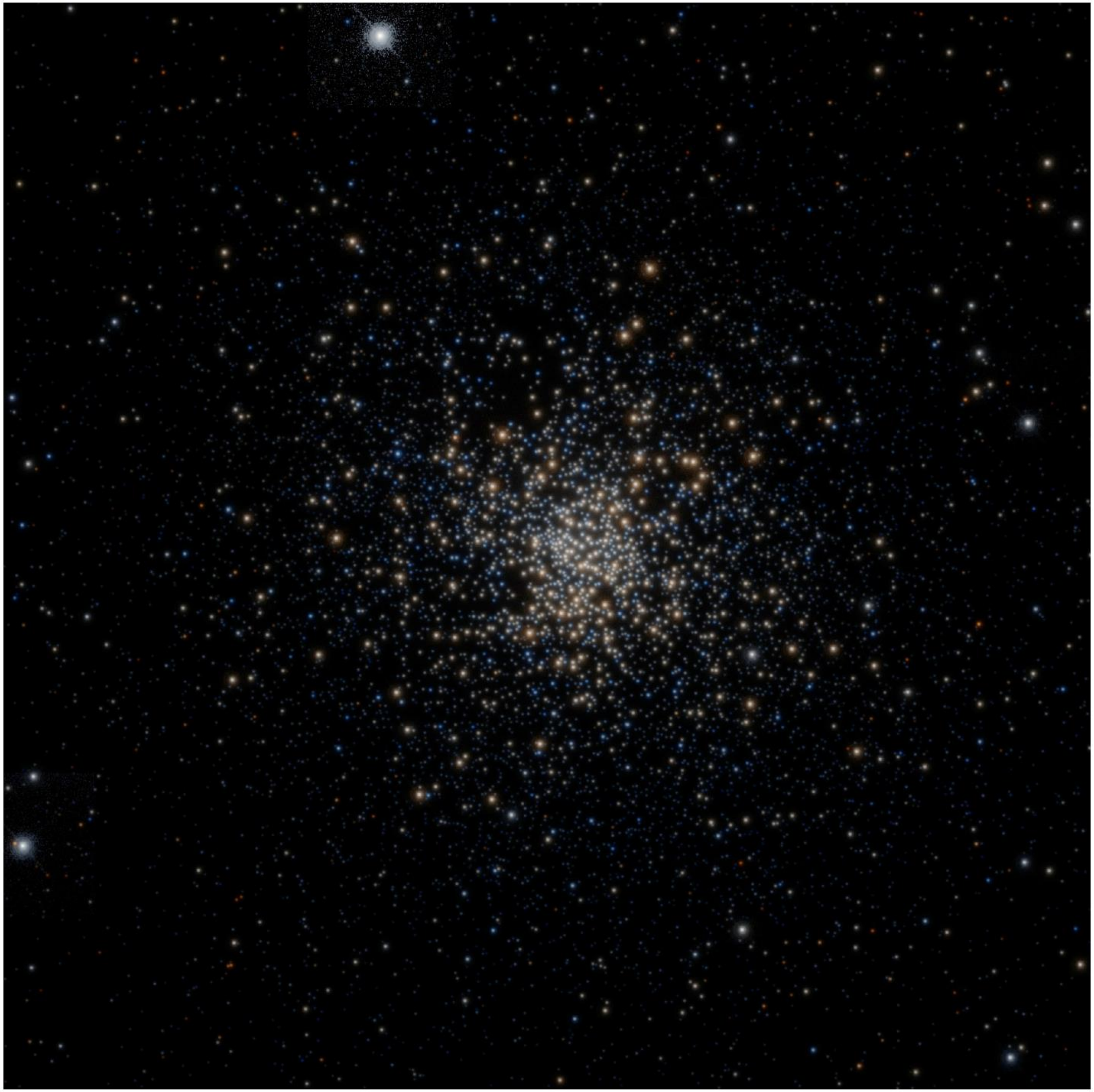

Rama Horizontal (HB)

- Dependencia con metalicidad
  - → se supone que, como las estrellas tienen ± la misma edad (las de misma masa alcanzan juntas el *RGB tip*) y la evolución durante el HB es muy rápida, las diferencias son en metalicidad (≠ pérdida de masa?)
- clases de Oosterhoff:
  - **I**: más rojas, con RRLyrae del tipo ab (<P)
  - **II**: mas azules, con RRLyrae del tipo c (>P)

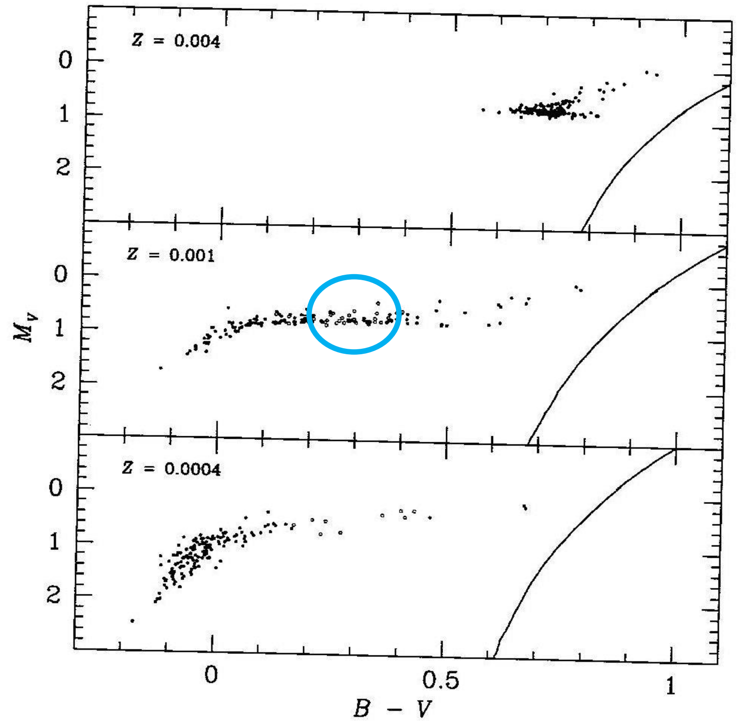

Figure 6.9 The HB morphologies for three simulated clusters with the metallicities indicated. All three clusters have the same age (13 Gyr) and helium abundance ($Y = 0.22$). Individual points show the predicted locations of stars which have undergone different amounts of mass loss as described in the text, and are currently evolving through their core helium burning phase. RR Lyrae stars are shown as open points. The line shows the location of the RGB from the isochrones in Green, Demarque & King (1987). [After Lee, Demarque & Zinn (1990) from data kindly supplied by Y.-W. Lee]

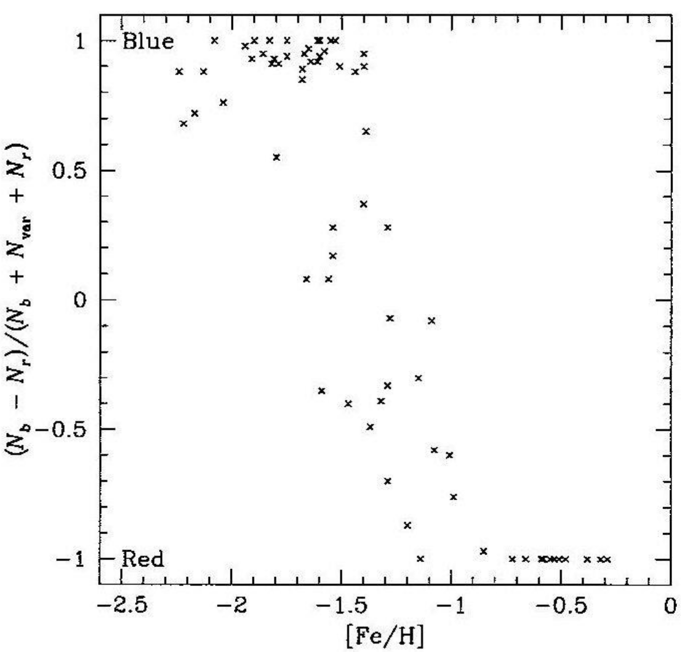

$$HB_{col} = (N_b - N_r) / (N_b + N_{var} + N_r)$$

Figure 6.4 Plot showing how the color of the HB in a globular cluster CM diagram varies with the cluster's metallicity. [After Lee (1990) from data kindly provided by Y.-W. Lee]

Distribución de metalicidades y edades

Distancias, edades e metalicidades

Métodos y escalas de distancia

- geométricos
- diagrama H-R
- variables pulsantes

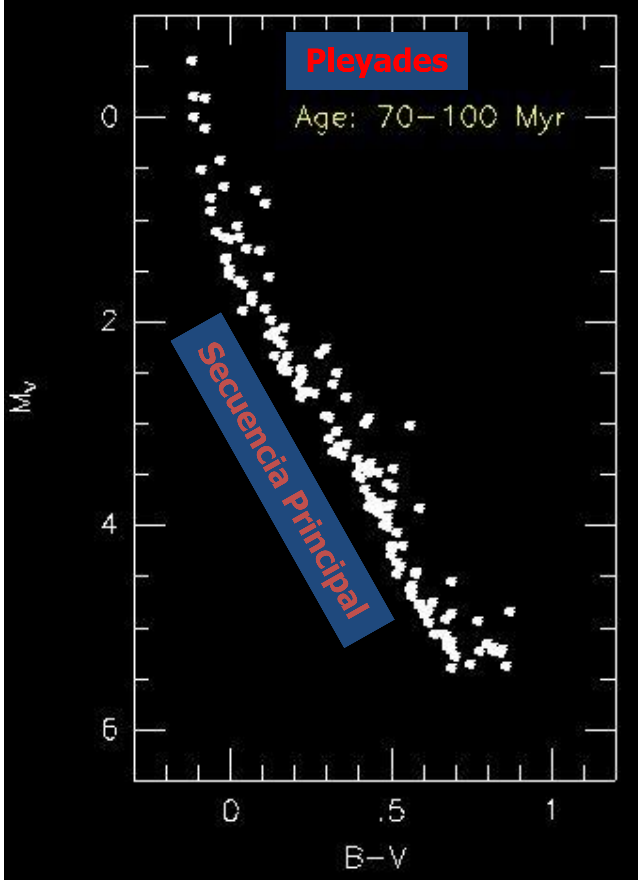

Estimación de edades

- absolutas
- relativas

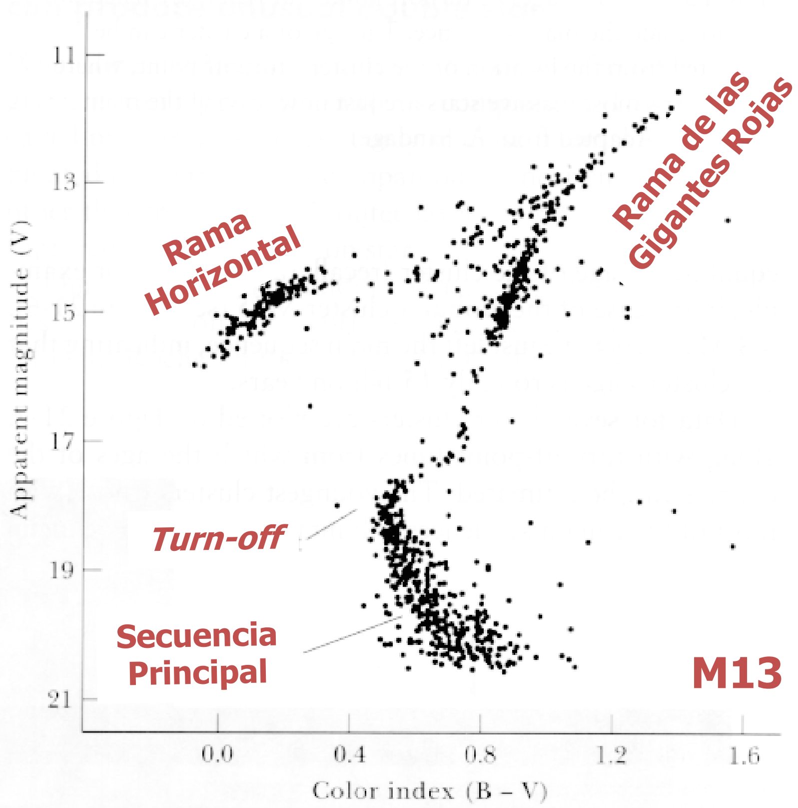

Estimación de metalicidades

- espectroscopia de alta resolución
- fotometría (DDO, *UBV)*

Métodos y escalas de distancia

	Aplicabilidad	
Geométricos		
• Paralaje trigonométrica (π)	CAb	
• Paralaje cinemática (grupos movientes)	CAb	
• Paralaje estadística (distancia astrométrica)	CAb	CGl
Diagrama H-R		
• Ajuste de la Secuencia Principal (ZAMS)	CAb	CGl (subenanas)
• Ajuste de la Rama Horizontal (HB)		CGl [M_V(RRLyr)]
• Ajuste de la secuencia de enfriamiento de las EB		CGl
Variables pulsantes		
• Baade-Wesselink		CGl
• RRLyrae (P-L)		CGl
• Cefeidas (P-L)	CAb	

Evolución de una población estelar en el Diagrama H-R

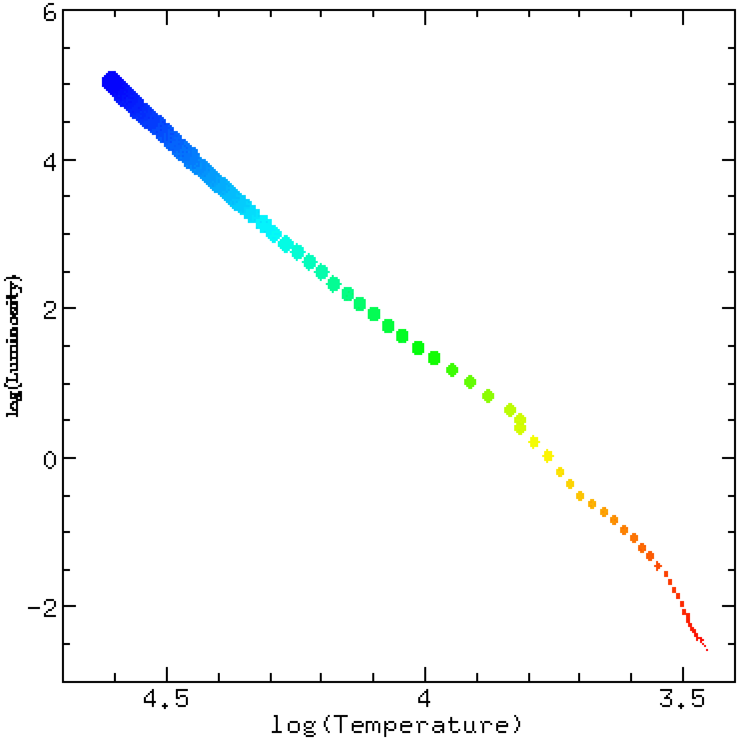

- Secuencia Principal de Edad Cero (ZAMS)

Isócronas

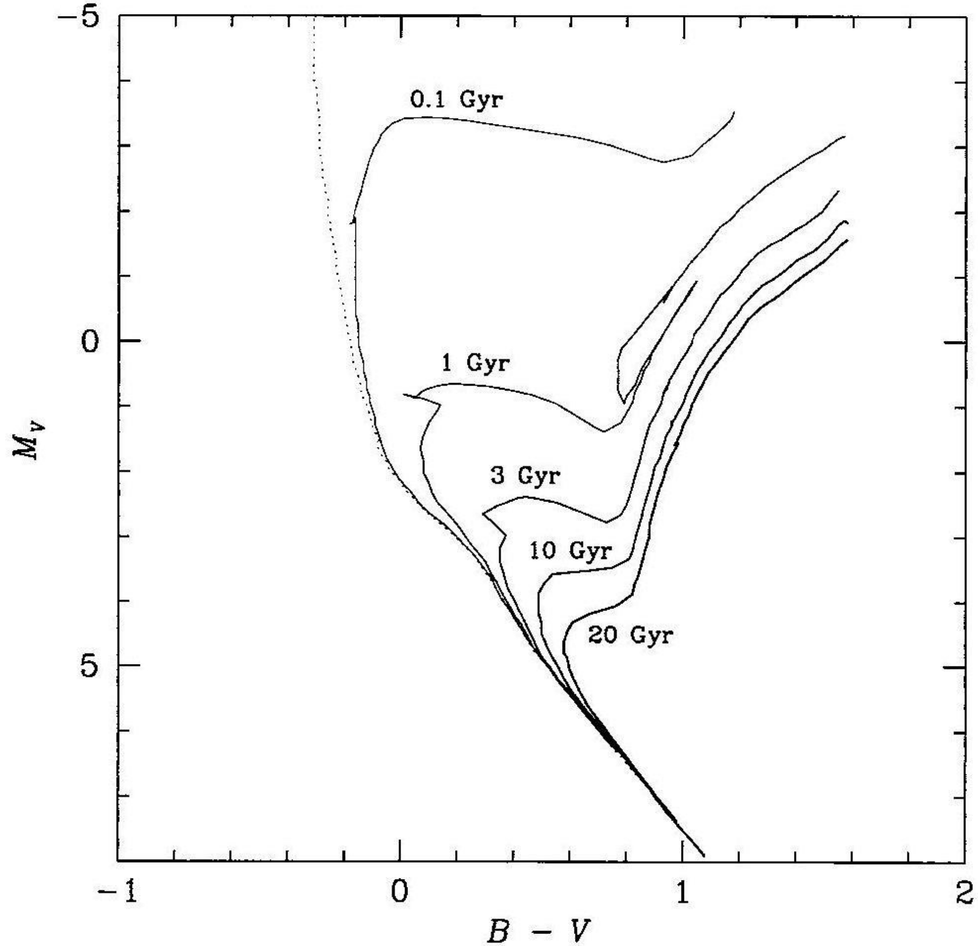

Figure 6.6 Theoretically calculated isochrones showing how a stellar population with $Z = 0.004$, $Y = 0.24$ evolves away from the ZAMS (dotted line) in the CM diagram. Each isochrones is labeled by its age. [From the calculations of Bertelli *et al.* (1994)]

Evolución de una población estelar en el Diagrama H-R

Isócronas

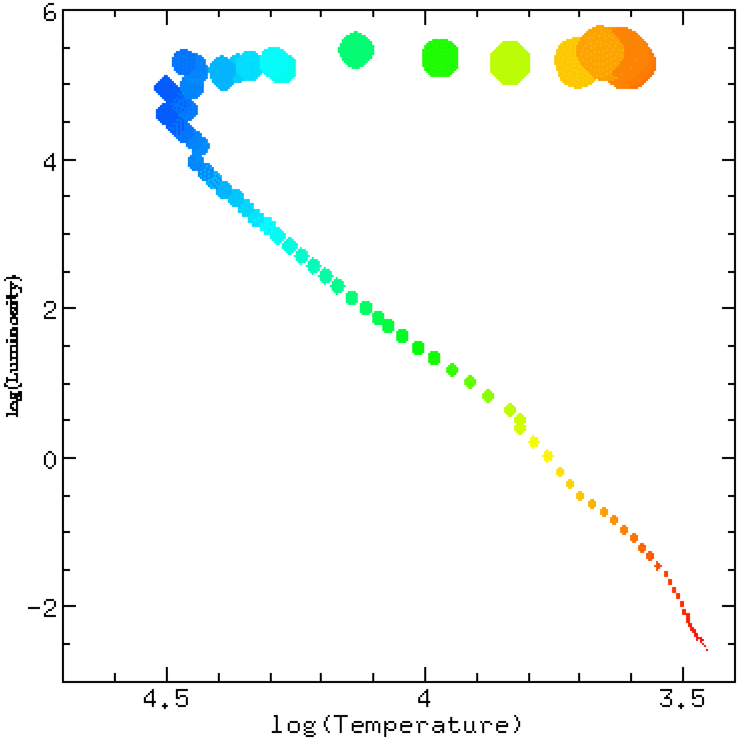

• 0.1 Gyr

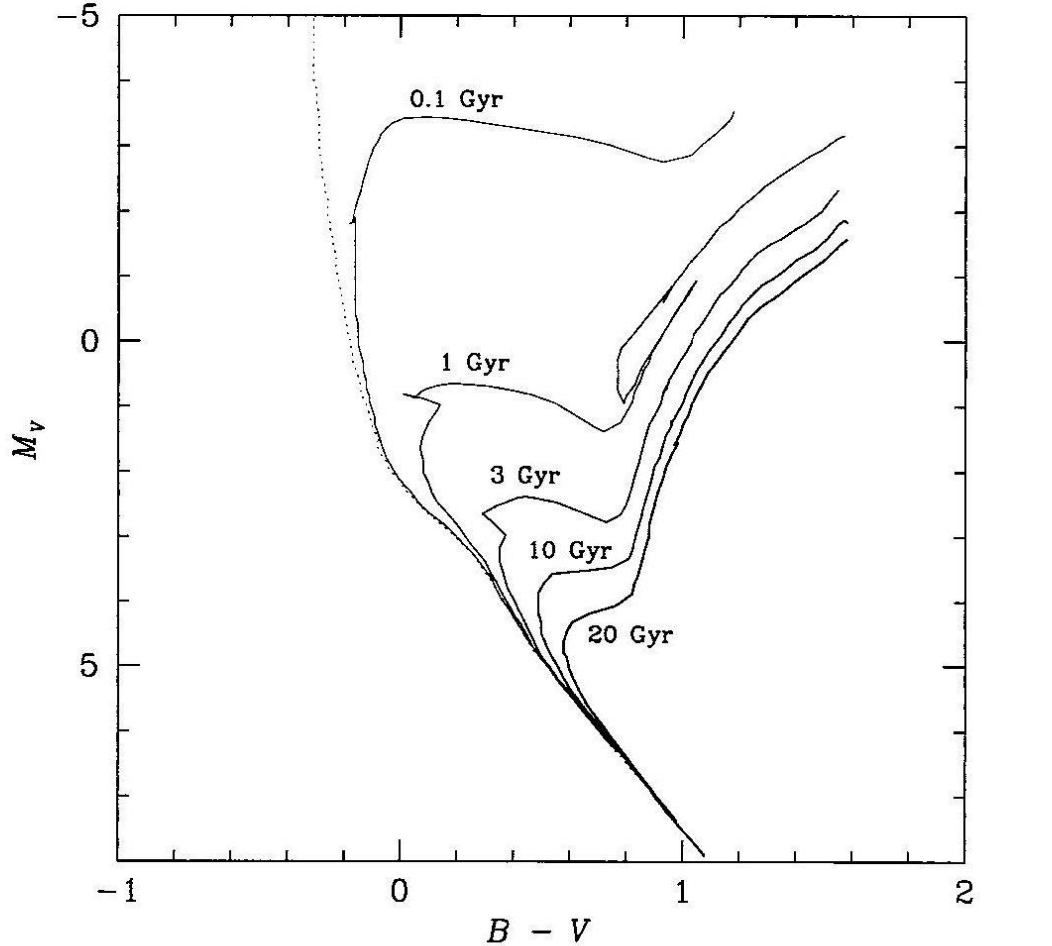

Figure 6.6 Theoretically calculated isochrones showing how a stellar population with $Z = 0.004$, $Y = 0.24$ evolves away from the ZAMS (dotted line) in the CM diagram. Each isochrones is labeled by its age. [From the calculations of Bertelli *et al.* (1994)]

Evolución de una población estelar en el Diagrama H-R

Isócronas

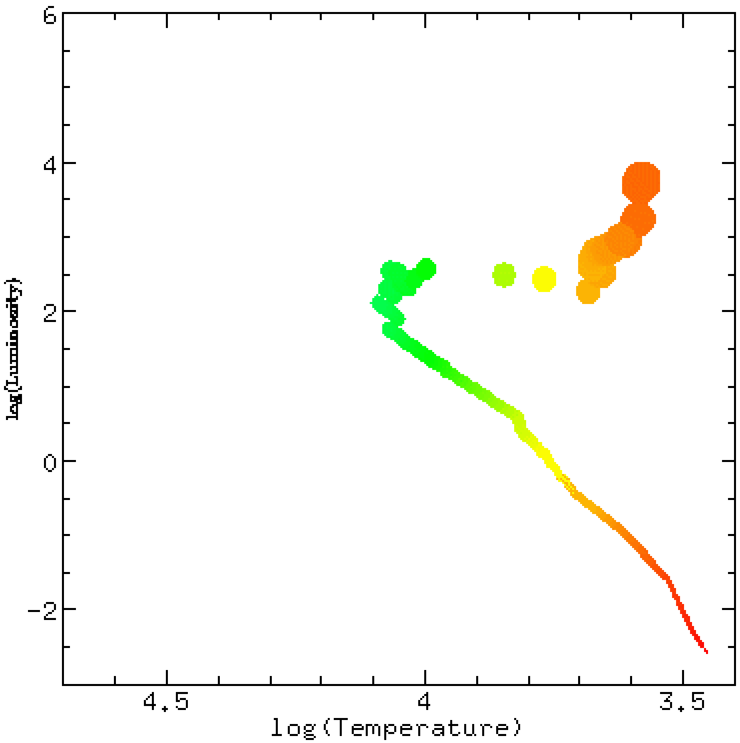

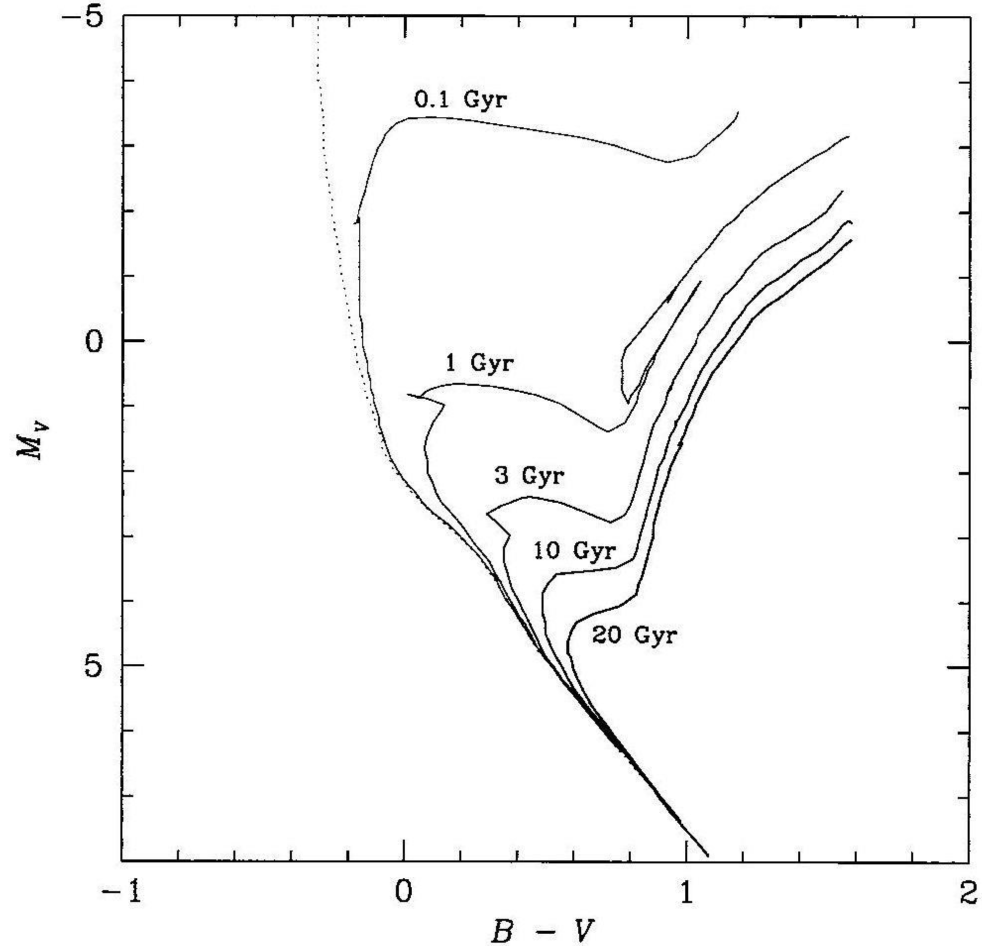

- 1 Gyr

Figure 6.6 Theoretically calculated isochrones showing how a stellar population with $Z = 0.004$, $Y = 0.24$ evolves away from the ZAMS (dotted line) in the CM diagram. Each isochrones is labeled by its age. [From the calculations of Bertelli *et al.* (1994)]

Evolución de una población estelar en el Diagrama H-R

Isócronas

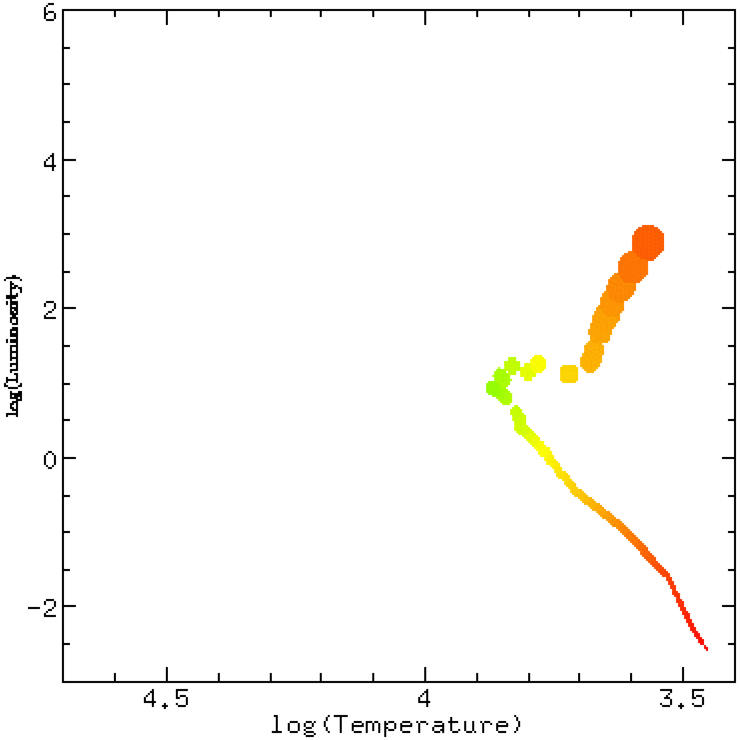

• 3 Gyr

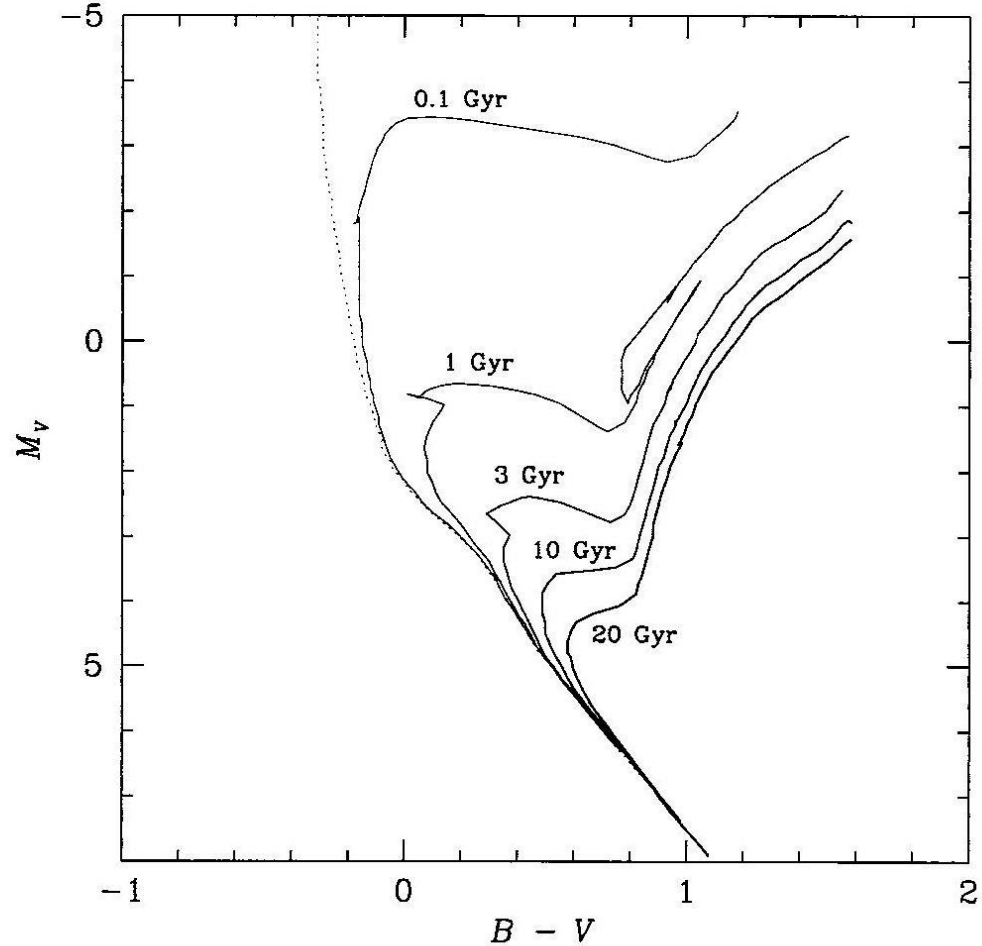

Figure 6.6 Theoretically calculated isochrones showing how a stellar population with $Z = 0.004$, $Y = 0.24$ evolves away from the ZAMS (dotted line) in the CM diagram. Each isochrones is labeled by its age. [From the calculations of Bertelli *et al.* (1994)]

Evolución de una población estelar en el Diagrama H-R

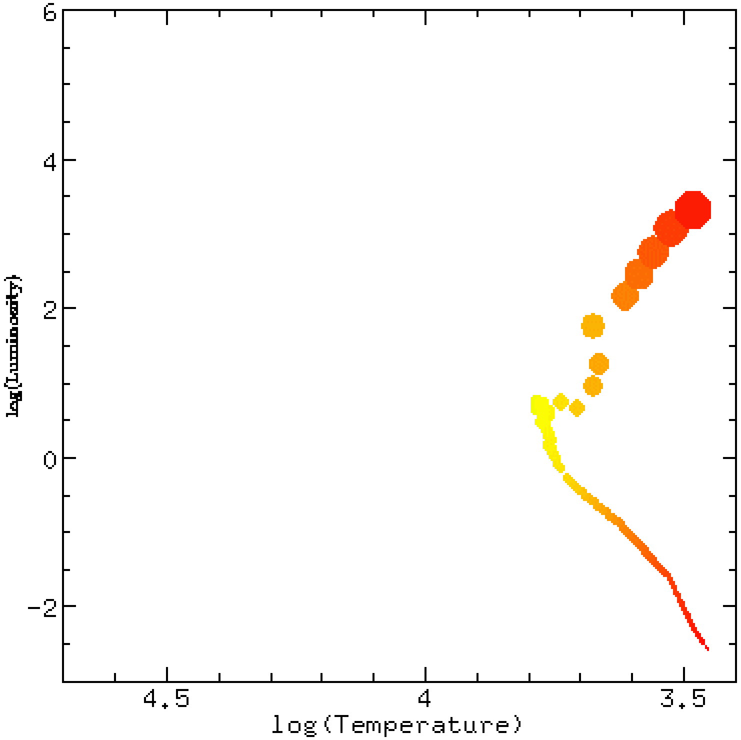

- 10 Gyr

Isócronas

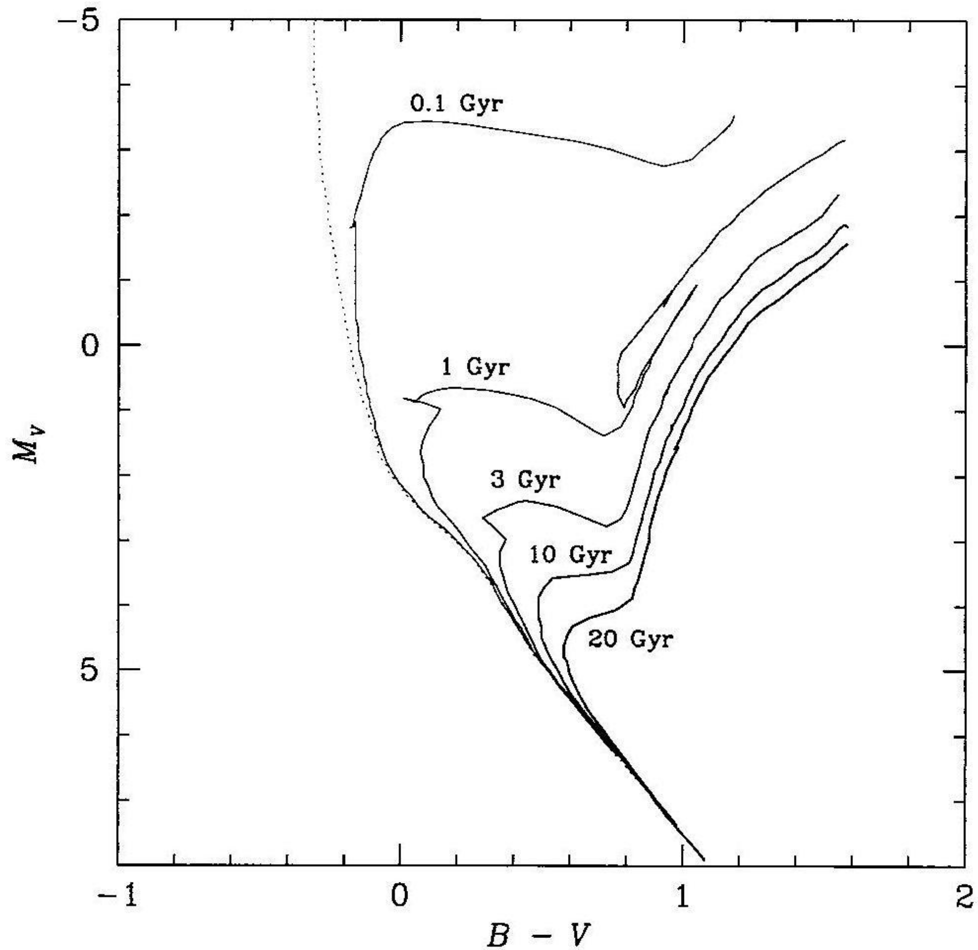

Figure 6.6 Theoretically calculated isochrones showing how a stellar population with $Z = 0.004$, $Y = 0.24$ evolves away from the ZAMS (dotted line) in the CM diagram. Each isochrones is labeled by its age. [From the calculations of Bertelli *et al.* (1994)]

Estimación de Edades

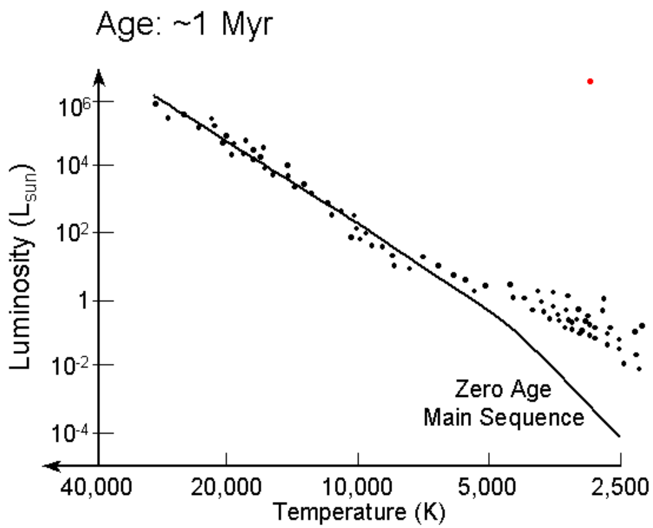

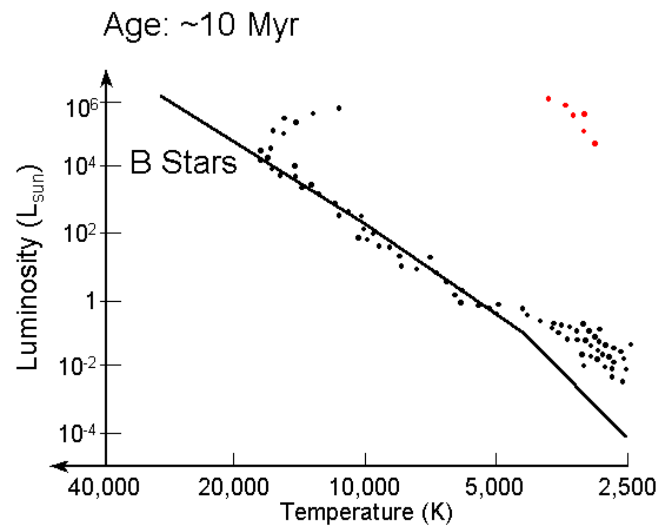

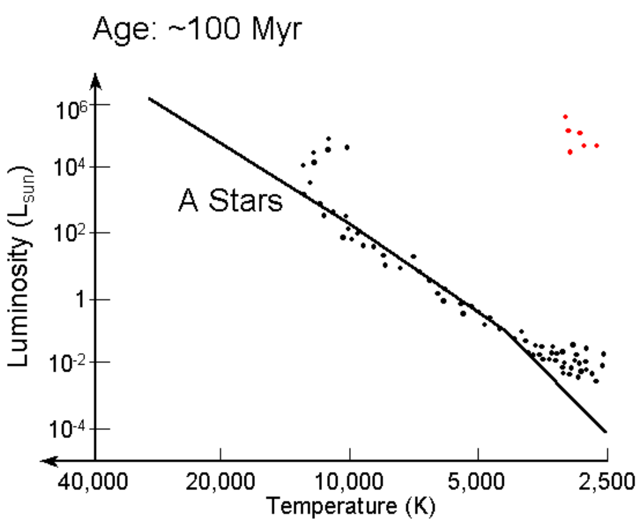

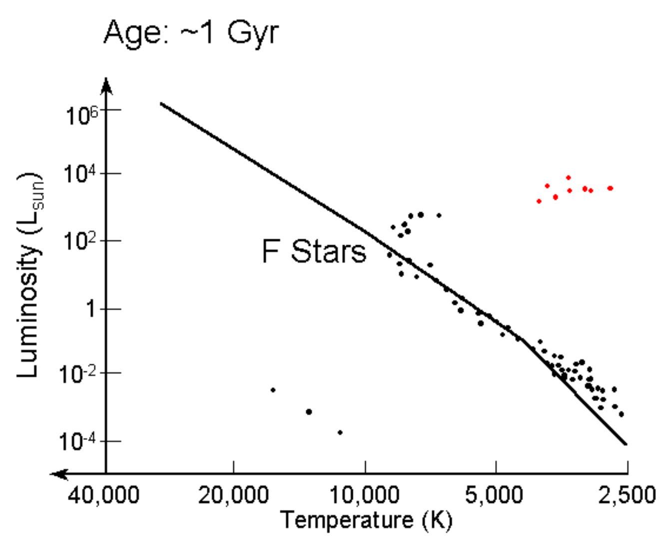

Isócronas

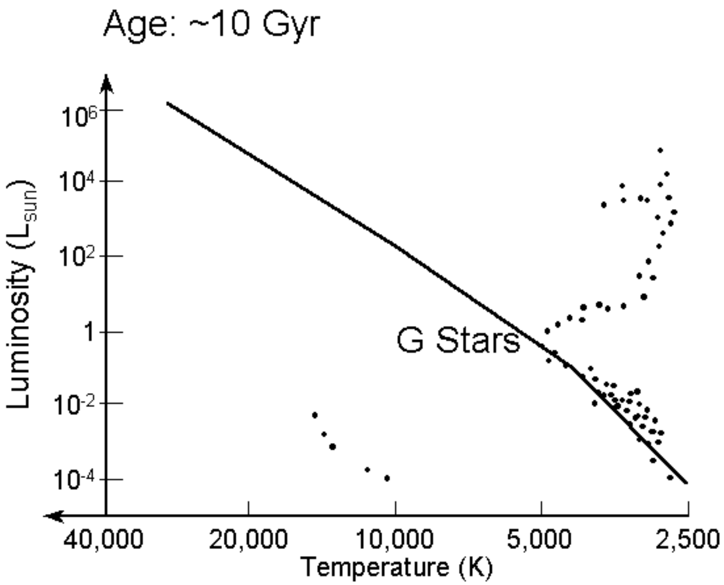

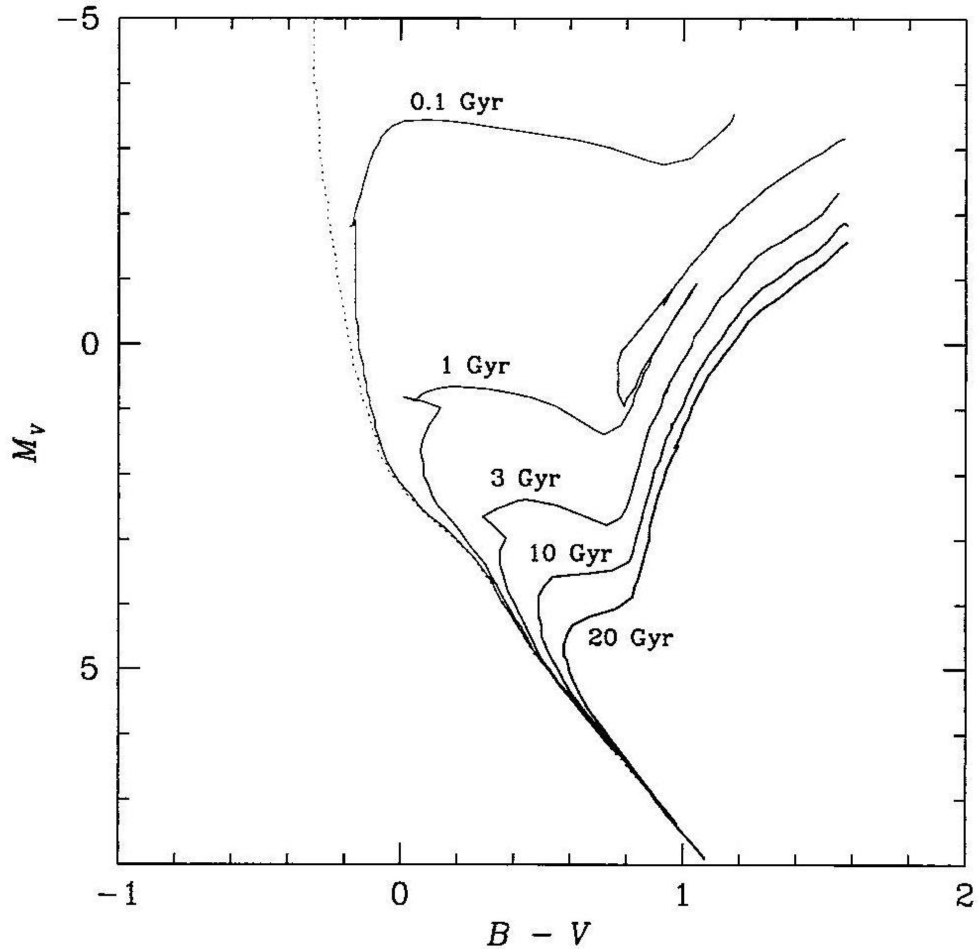

Figure 6.6 Theoretically calculated isochrones showing how a stellar population with $Z = 0.004$, $Y = 0.24$ evolves away from the ZAMS (dotted line) in the CM diagram. Each isochrones is labeled by its age. [From the calculations of Bertelli *et al.* (1994)]

Estimación de Edades

- Ajuste de isócronas
- Punto de *turn-off*

$$M_V^{TO} = 2.70 \log(t_{Ga}) + 0.30\,[Fe/H] + 1.41$$

- Método ΔV

$$M_V^{HB} = 0.17\,[Fe/H] + 0.82$$

$$\Delta V = M_V^{TO} - M_V^{HB} = 2.70 \log(t_{Ga}) + 0.13\,[Fe/H] + 0.59$$

- Método Δ(B–V)

$$\Delta(B-V) = (B-V)_{SGB} - (B-V)_{TO}$$

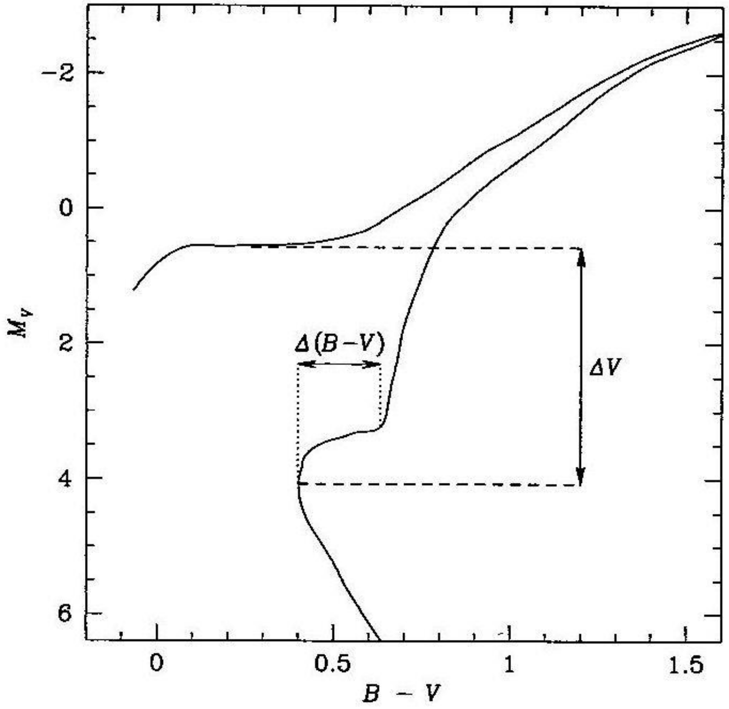

Figure 6.11 Illustration of the distance-independent age diagnostics, ΔV and $\Delta(B-V)$, as calculated from the principal sequences in the CM diagram for a typical globular cluster.

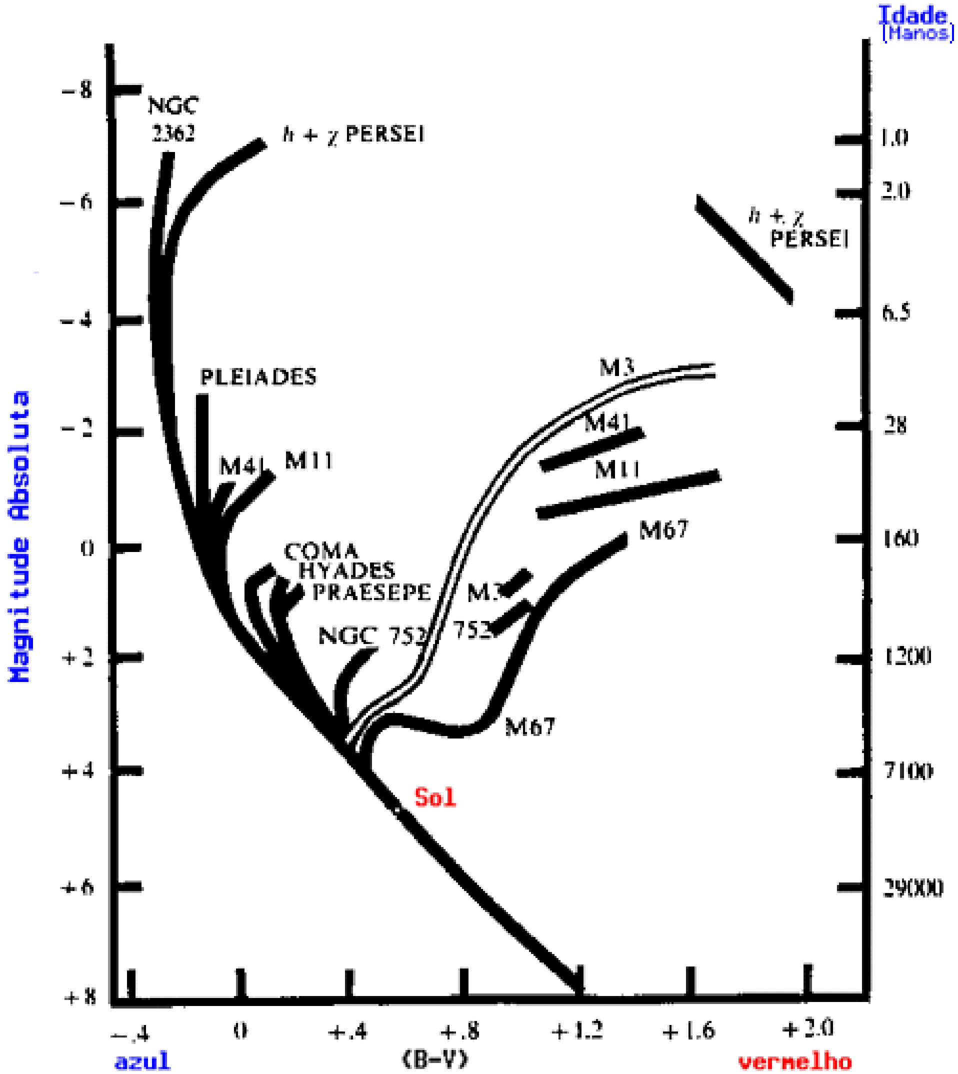

- Ajuste de isócronas
- Punto de *turn-off*

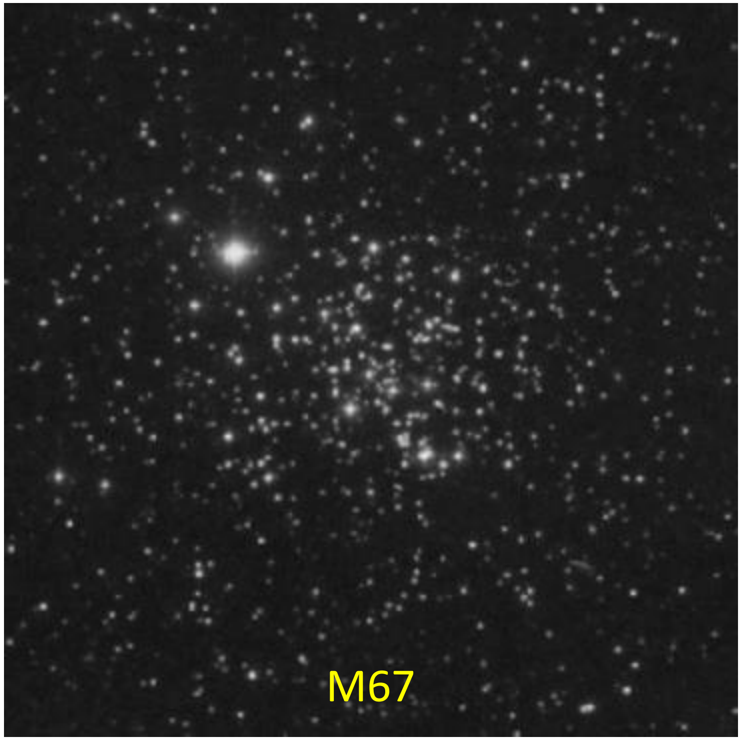

Metalicidades

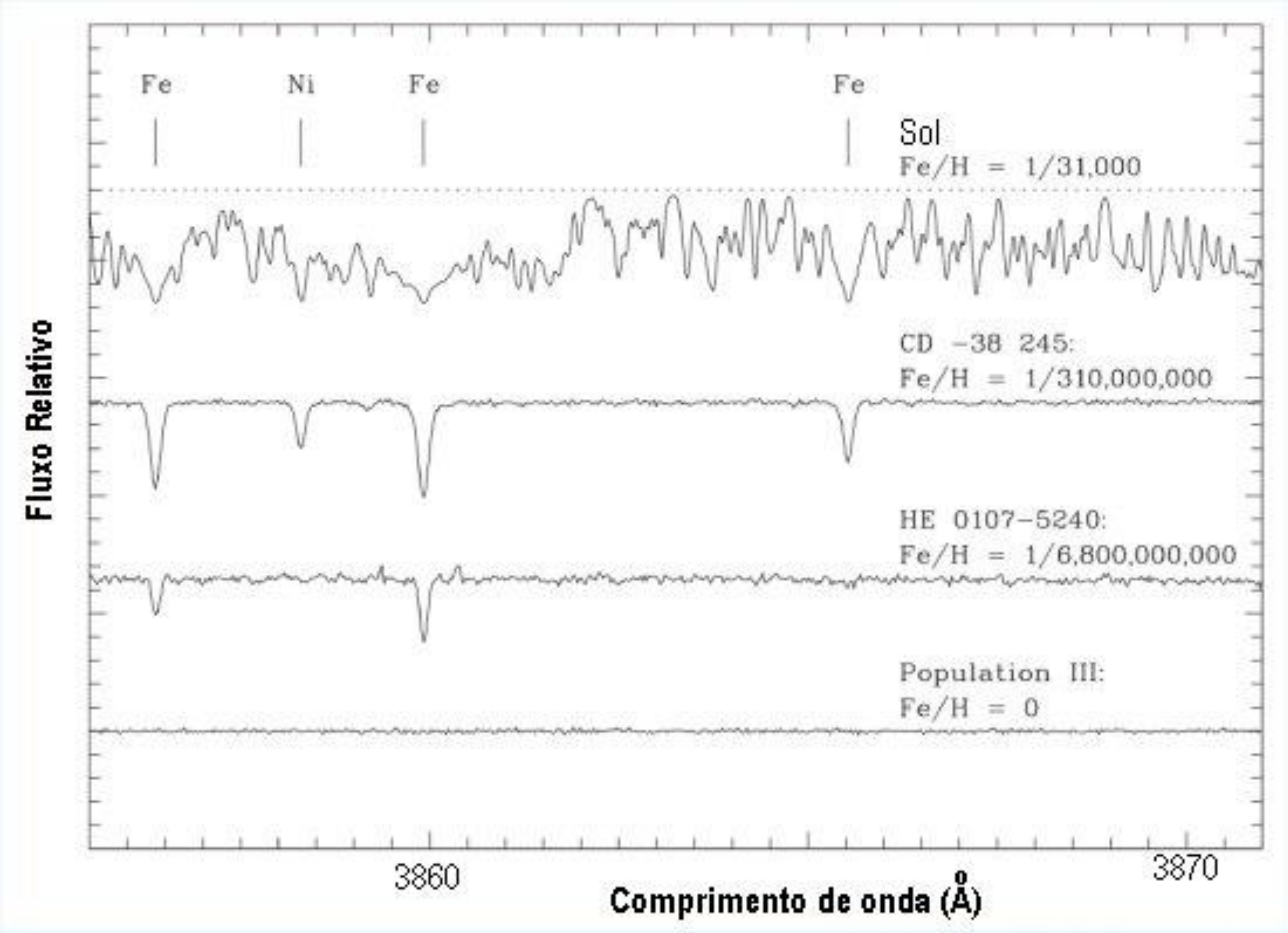

Metalicidades

Chen et al. (2003),
AJ 125, 1397

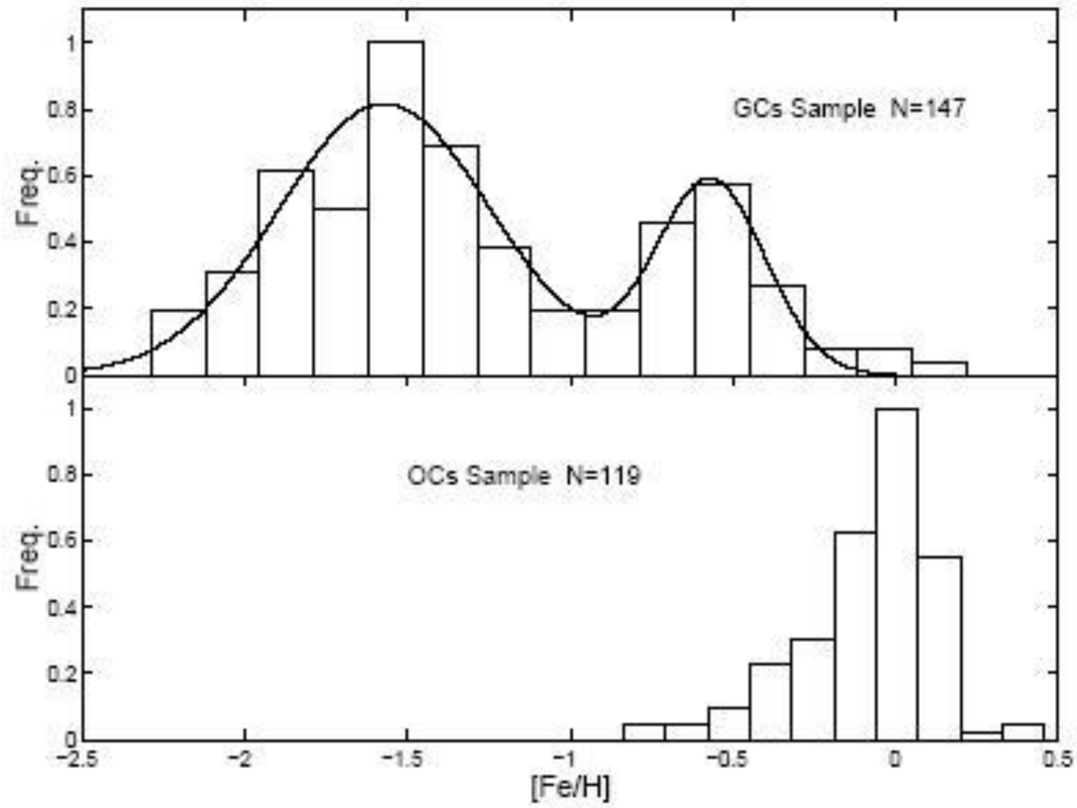

FIG. 6.—Comparison of the metallicity distributions for Galactic globular and open clusters.

perfil radial

Perfiles Radiales

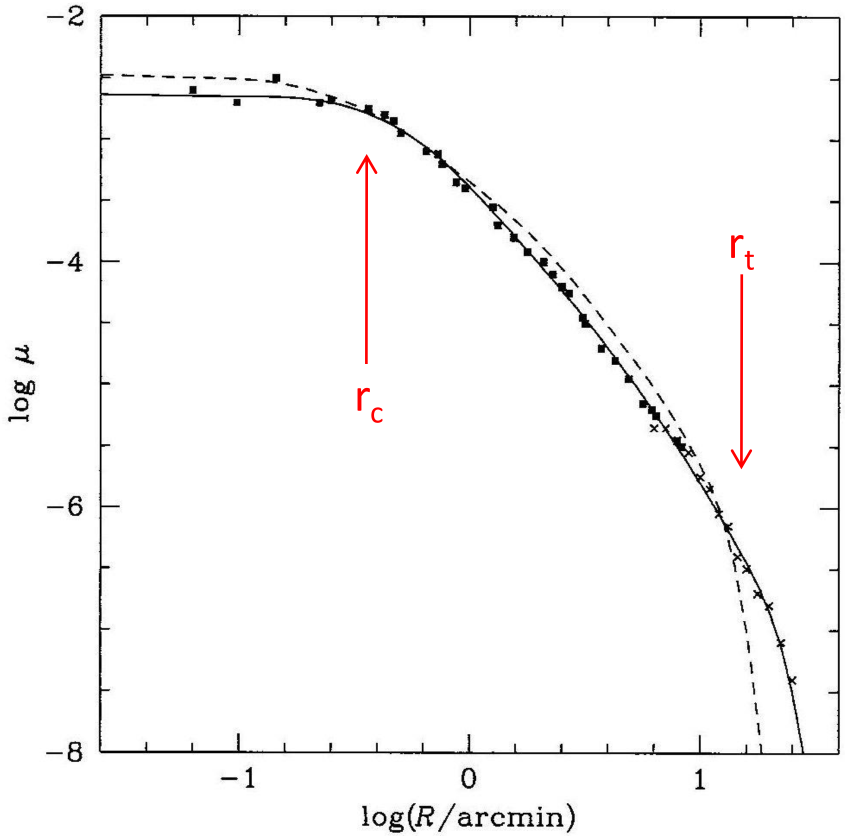

Figure 6.18 plot of surface brightness, μ, versus projected radius for the globular cluster M3. The profile at small radii (solid symbols) is derived from integrated photometry, while that at large radii (crosses) is derived from star counts. The dashed line shows the King model which best fits these data, and the solid line shows a more sophisticated multi-mass King model fit. [After Da Costa & Freeman (1976)]

- Modelos de King (masas múltiples)

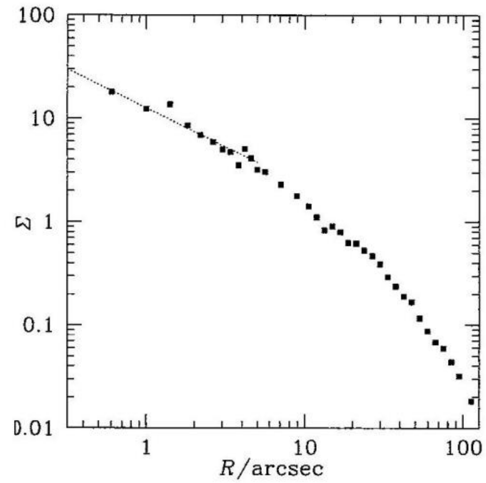

Figure 6.22 The surface density of stars brighter than $m_V = 19$ as a function of projected radius in the globular cluster M15, as derived from a HST image (Guhathakurta *et al.* 1996). The dotted line shows a surface-brightness profile with a power law of index −0.75, as would be expected for the if the cluster contained a central massive black hole. [From data kindly provided by R. Guhathakurta]

- *core* (carozo/hueso, región central)
  - → *flat core* (achatado, 80%)
  - → *cuspy core* (empinado, 20%)
    - colapso del carozo
    - agujero negro masivo

dinámica y evolución

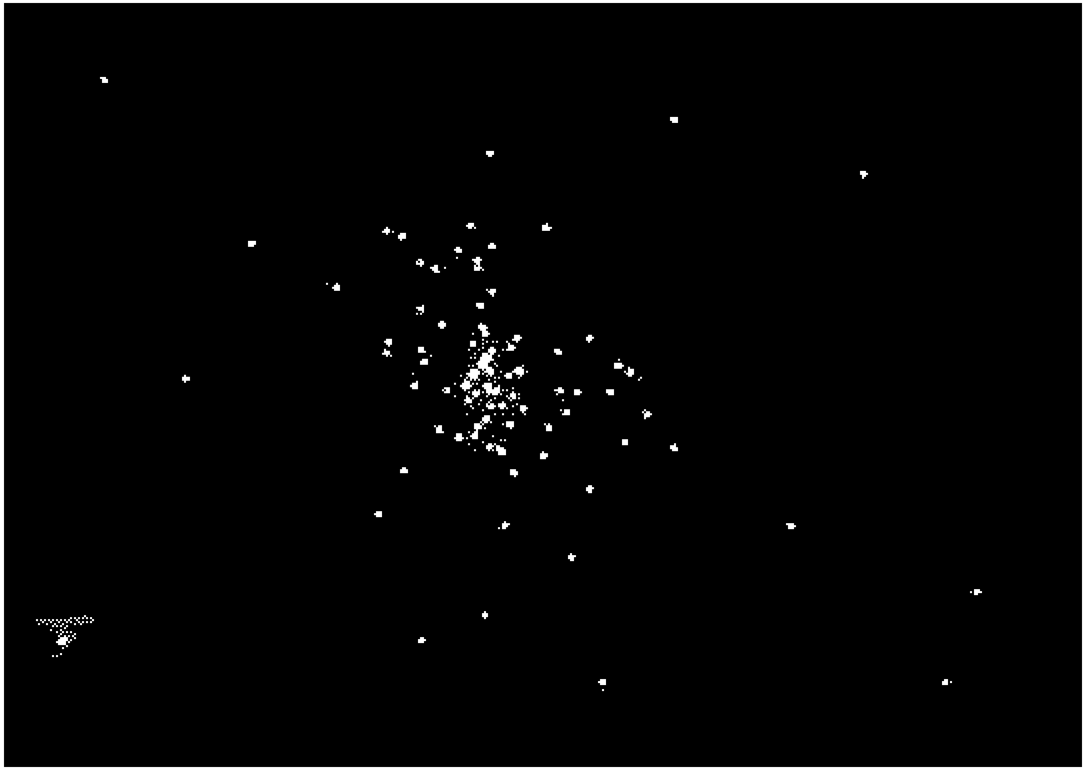

Dispersión de velocidades

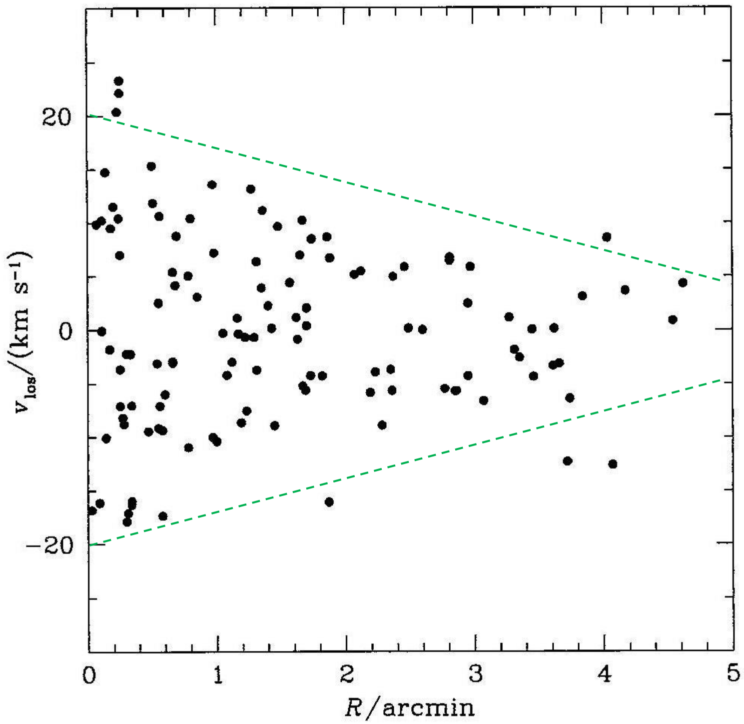

Figure 6.23 Line-of-sight velocities of giant stars in M15 as a function of their projected radii. [From data published in Peterson, Seitzer & Cudworth (1989)]

Movimientos propios

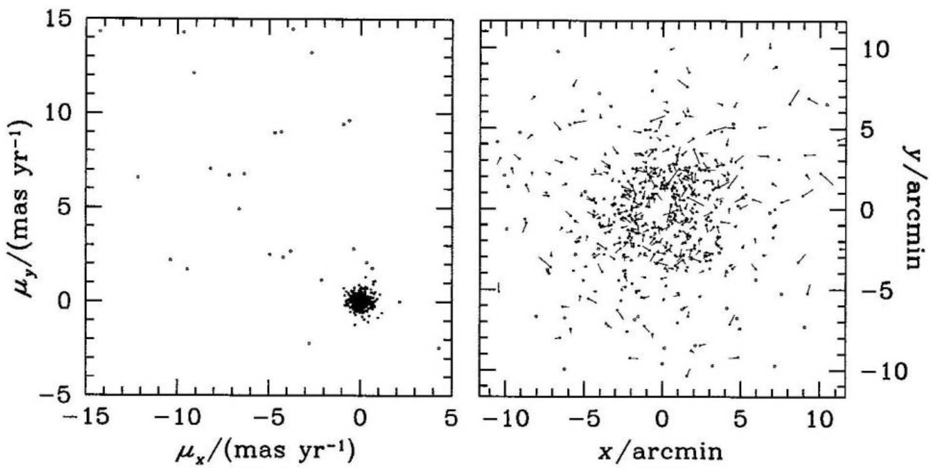

Figure 6.24 Proper motions of stars in the field containing the globular cluster M5. The left panel shows the angular velocity for each star, $\{\mu_x, \mu_y\}$; the stars identified as cluster members are shown as solid points, while field stars are marked by open circles. The right panel shows the locations of these stars on the sky, with lines marking where the proper motions predict that the cluster members will have moved to in 5×10^4 years. Proper motions have not been determined at small radii due to crowding. [From data published in Rees (1993)]

IMF

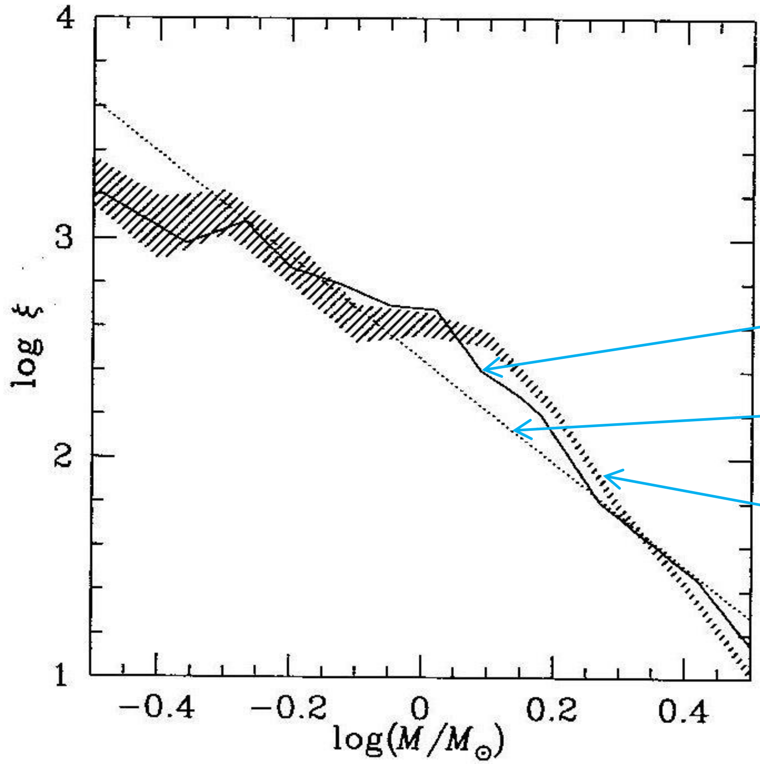

Figure 6.31 The initial mass function for the Pleiades, as derived by Meusinger, Schilbach & Souchay (1996) (solid line) compared to the simple Salpeter IMF of equation (5.14) (dotted line) and the IMF derived by Basu & Rana (1992) for the solar neighborhood (shaded region). The IMFs have been normalized to agree at $2\,\mathcal{M}_\odot$. The uncertainty in the solar neighborhood IMF arises from the uncertain history of star formation in the Galaxy.

List of some IMFs used in cosmology: Salpeter '55 eq. 5; Miller & Scalo '79 table 7; Kennicutt '83 section V; Scalo '86 table; Kroupa, Tout & Gilmore '93 eq. 13; Kroupa '01 eq. 2; Baldry & Glazebrook '03 abstract; Chabrier '03 table 1.

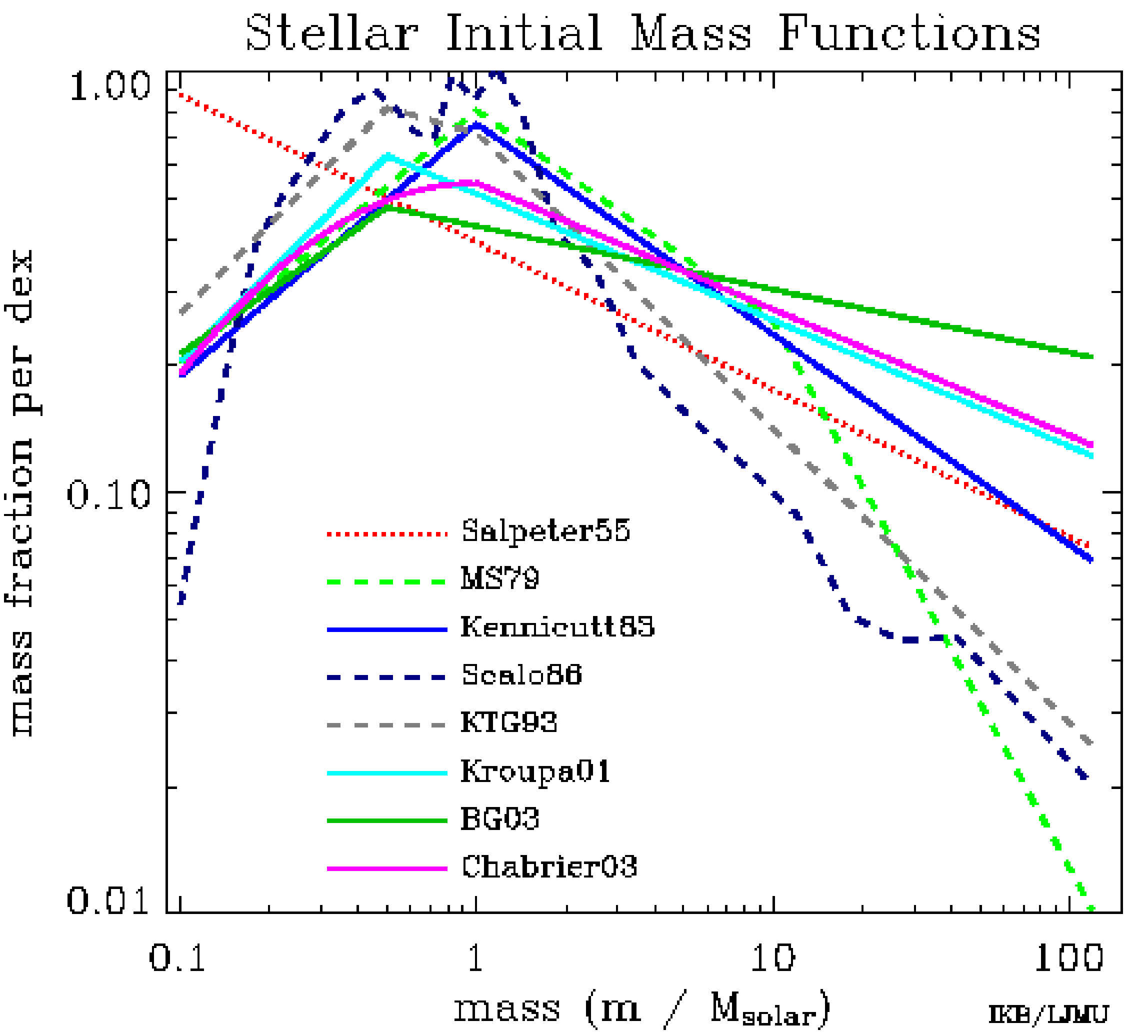

This figure compares the IMFs by ploting mass fraction per dex versus mass, i.e., normalized so that the integral under each curve is unity. They are assumed to be valid from 0.1 to 120 solar masses.

http://www.astro.ljmu.ac.uk/~ikb/research/imf-use-in-cosmology.html

Evolución de la dinámica interna

Relajación dinámica

Mecanismos de disolución

	CAb	CGl
✧ procesos internos		
• evaporación	X	X
• pérdida de masa por la evolución estelar	X	X
✧ procesos externos		
• choque con el disco		X
• choque con nubes interestelares	X	
• efecto de marea de la Galaxia	X	X
• fricción dinámica	X	X
• difusión de estrellas de campo	X	

Mecanismos de disolución

Procesos internos

▷ **evaporación**

relajación dinámica → acercamiento de la equipartición de E_C

→ $< M_\star \Rightarrow > v_\star$ → $v_\star > v_{esc}$

→ E_{lig} disminuí → v_{esc} disminuí → mas ☆ escapan

▷ **pérdida de masa por la evolución estelar**

$\left.\begin{array}{l}\text{explosión de SNe}\\ \text{eyección de PNe}\\ \text{viento estelar}\end{array}\right\}$ también disminuí E_{lig}

→ mas crítica para ☆ mas masivas ⇒ mas crítico para CAb + jóvenes

→ disrupción total por explosión de SN también es posible

Mecanismos de disolución

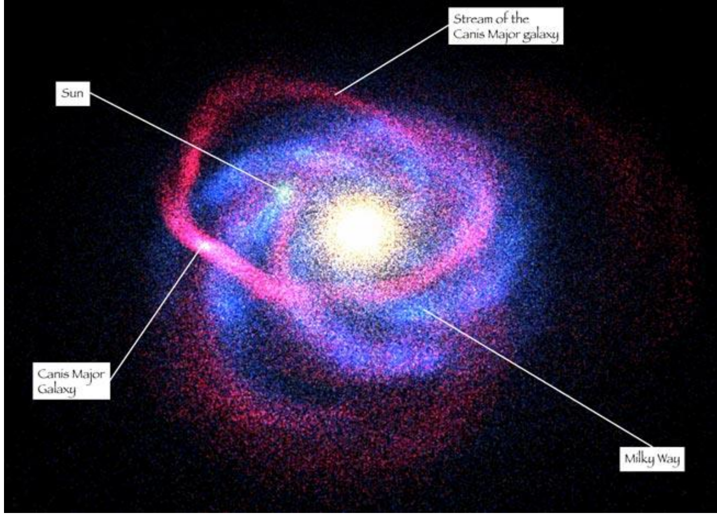

Procesos externos

▷ **choque con el disco de la Galaxia**

compresión → energía orbital para energía interna → evaporación

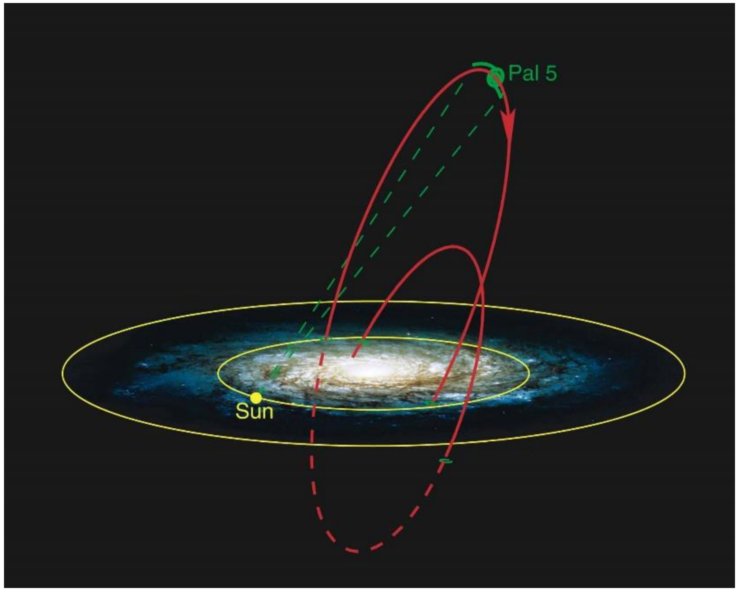

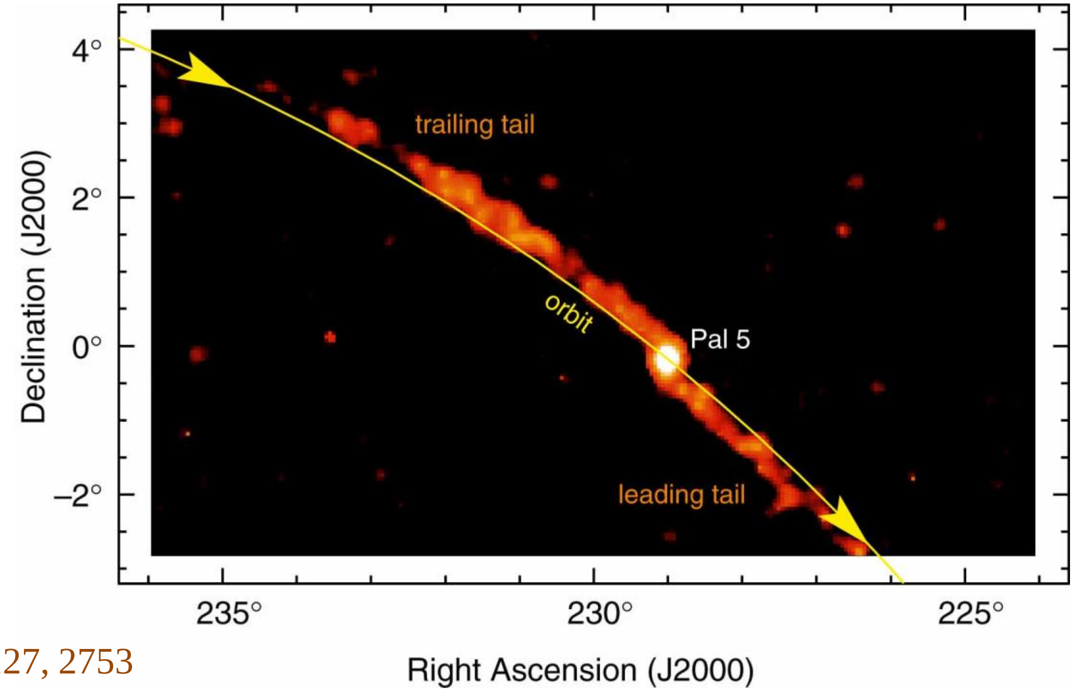

e.g. Dehnen et al. (2004), AJ 127, 2753

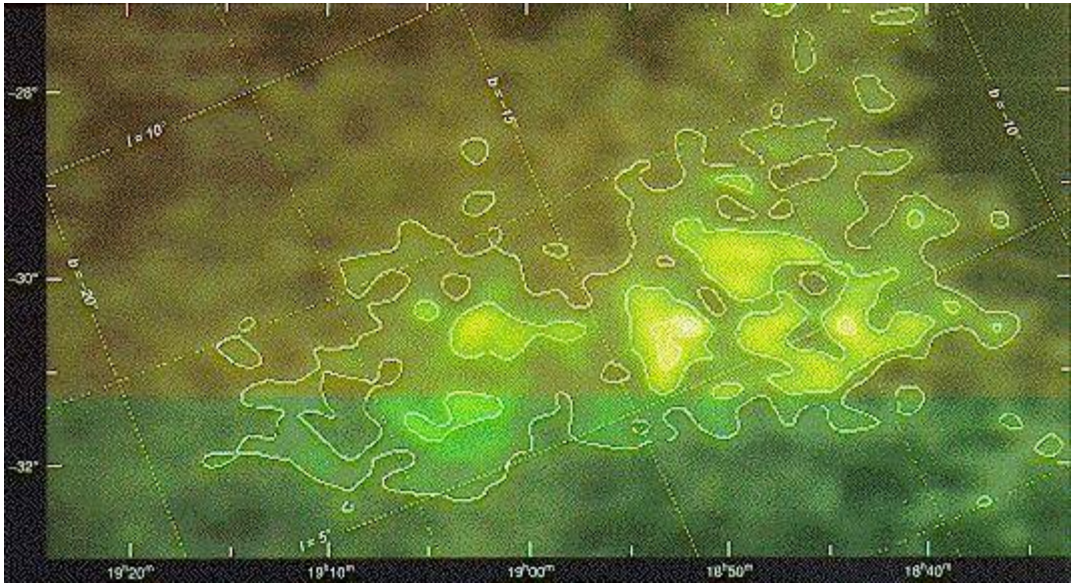
-28°
-30°
-32°
19h20m
19h10m
19h00m
18h50m
18h40m

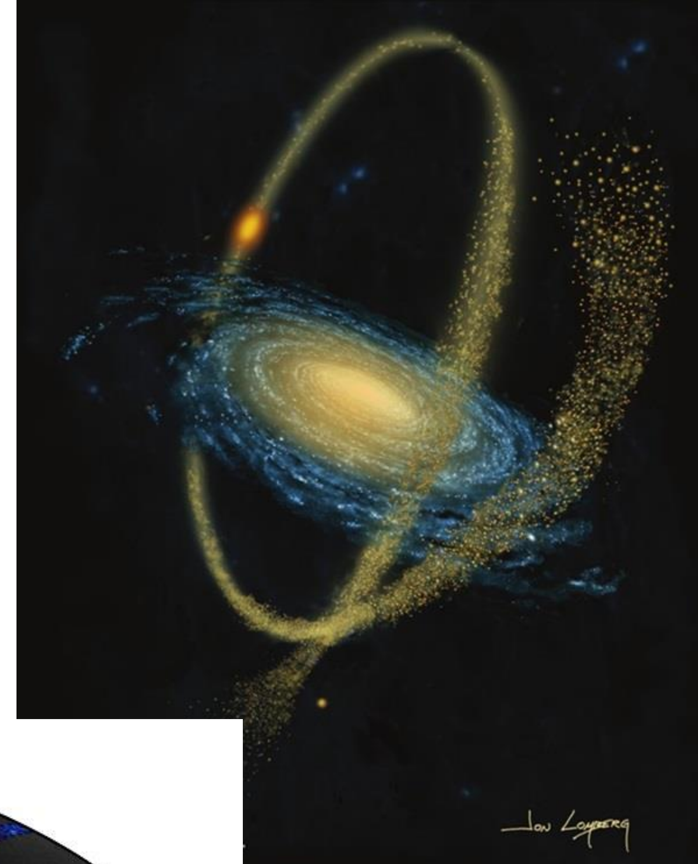

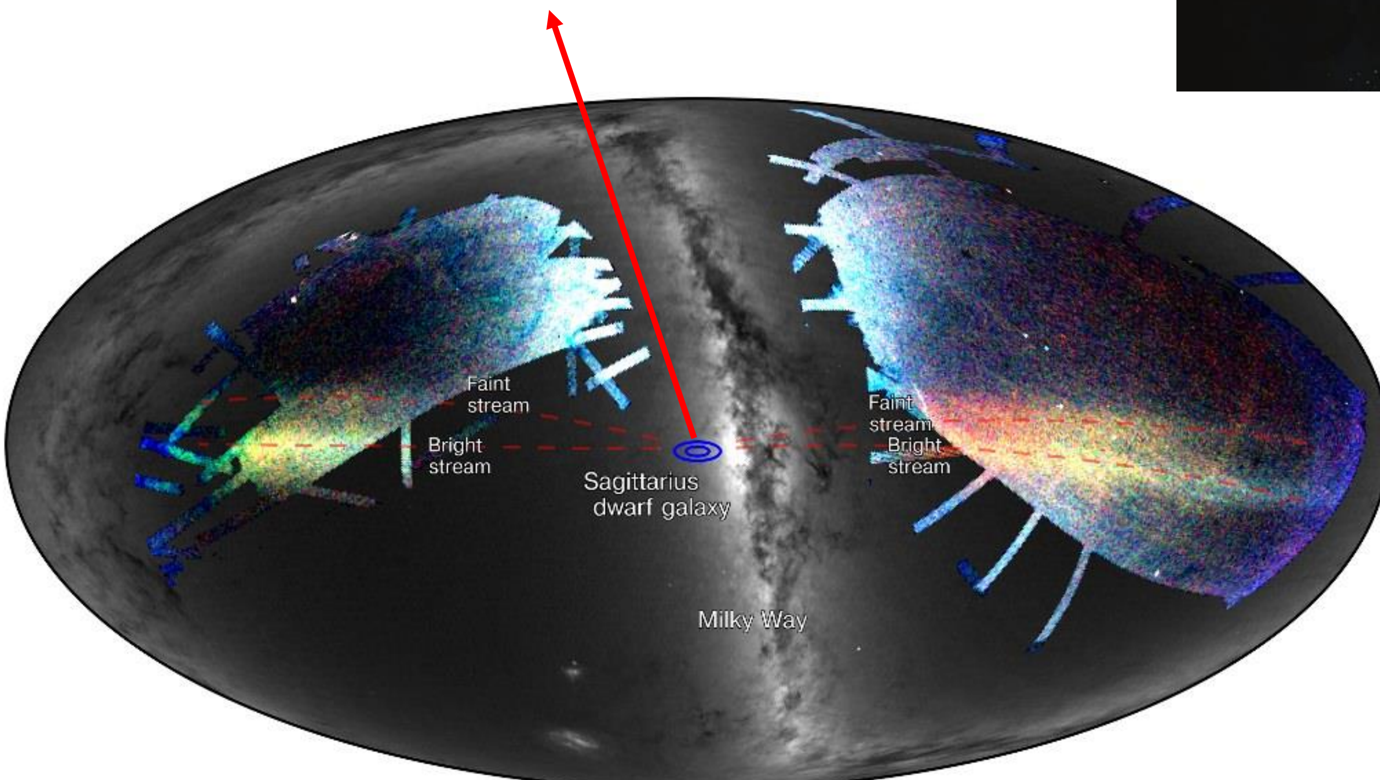
Faint
stream
Bright
stream
Sagittarius
dwarf galaxy
Faint
stream
Bright
stream
Milky Way

Mecanismos de disolución

Procesos externos

▷ **choque con el disco de la Galaxia**
compresión → energía orbital para energía interna → evaporación

▷ **choque con nubes interestelares**
mismo efecto
CAb pueden ser destruidos por choques repetidos

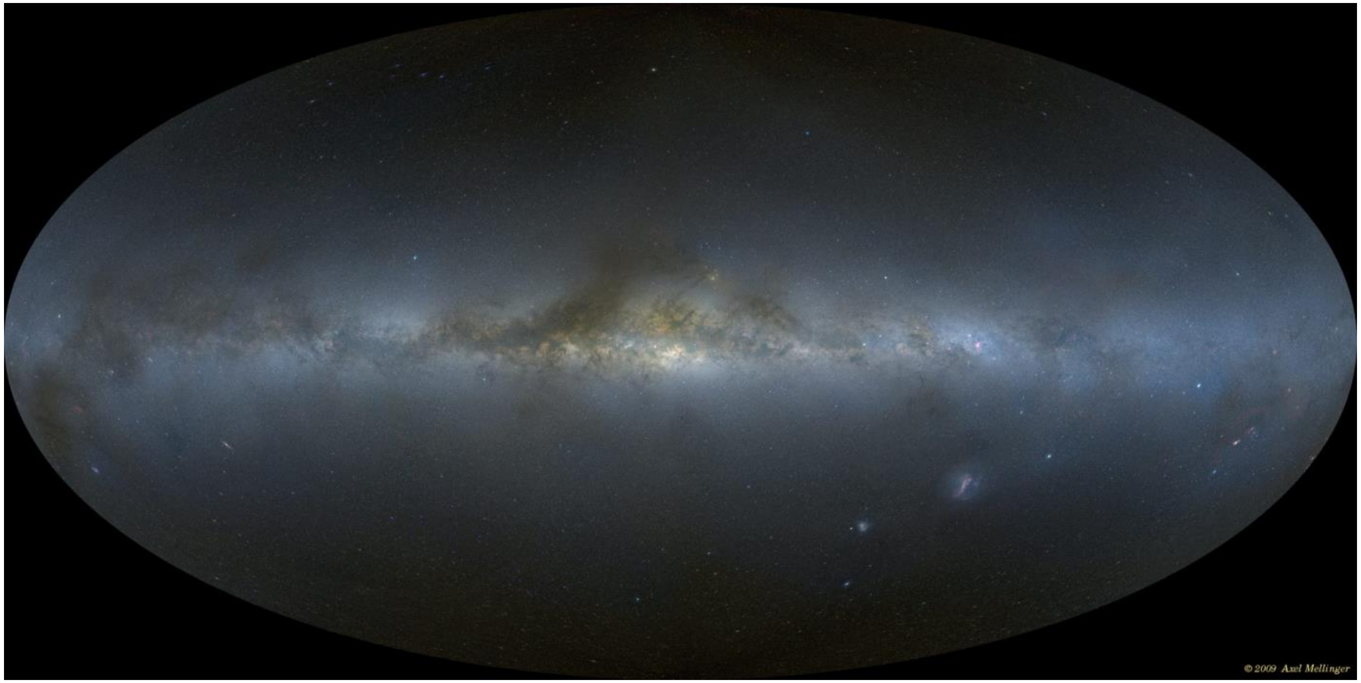

Mecanismos de disolución

Procesos externos

▷ **choque con el disco de la Galaxia**

compresión → energía orbital para energía interna → evaporación

▷ **choque con nubes interestelares**

mismo efecto

CAb pueden ser destruidos por choques repetidos

▷ **efecto de marea de la Galaxia (*tidal stripping*)**

el potencial Galáctico puede “arrancar” ☆ que alcanzan el r_t con energía suficiente

Mecanismos de disolución

Procesos externos

▷ **choque con el disco de la Galaxia**

compresión → energía orbital para energía interna → evaporación

▷ **choque con nubes interestelares**

mismo efecto

CAb pueden ser destruidos por choques repetidos

▷ **efecto de marea de la Galaxia (*tidal stripping*)**

el potencial Galáctico puede "arrancar" ☆ que alcanzan el r_t con energía suficiente

▷ **fricción dinámica**

el cúmulo pierde energía orbital para las ☆ y DM de la Galaxia (y espirala en dirección al CG) ⇒ estímulo a evaporación y efecto de marea

Dynamical Friction I

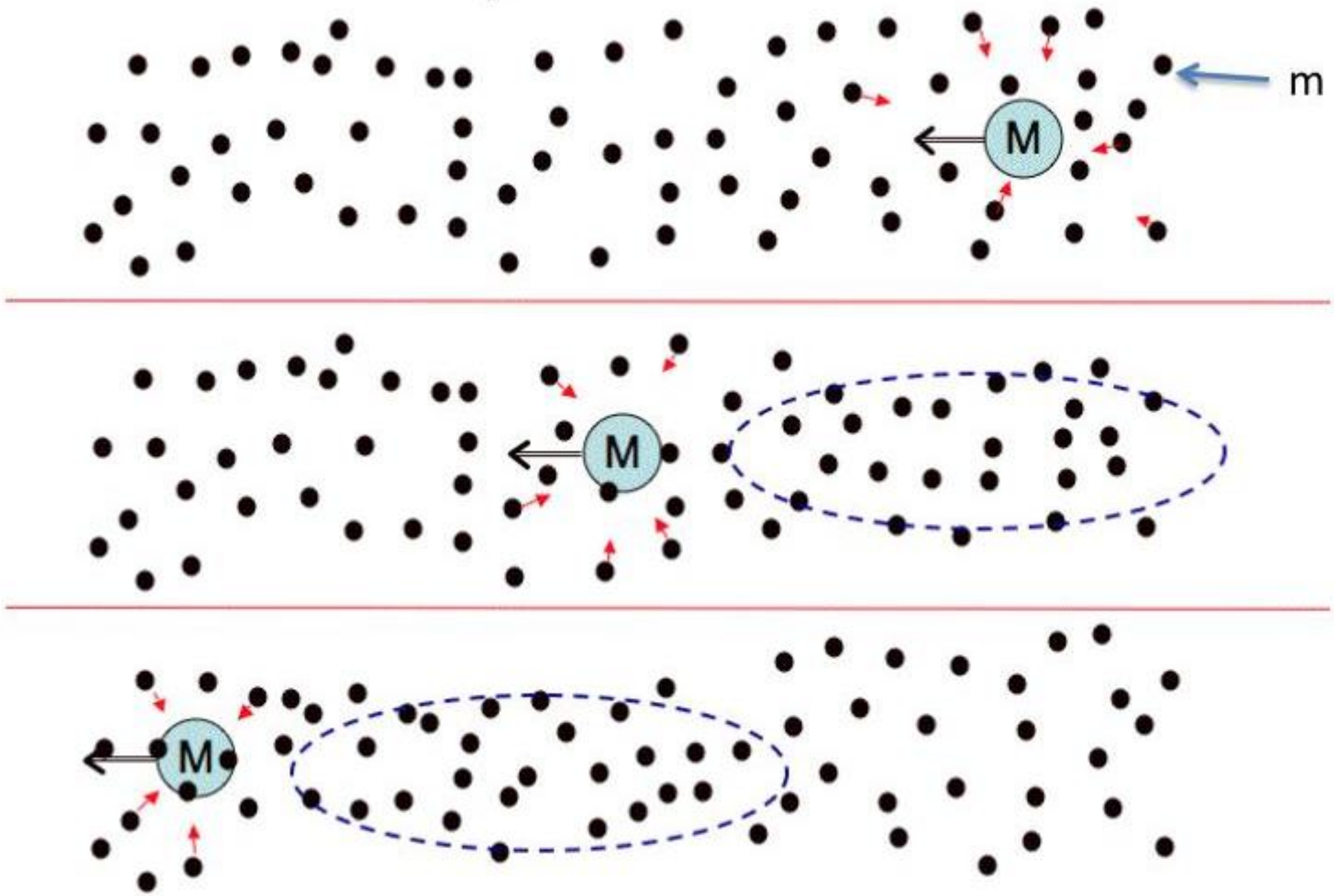

Mecanismos de disolución

Procesos externos

▷ **choque con el disco de la Galaxia**

compresión → energía orbital para energía interna → evaporación

▷ **choque con nubes interestelares**

mismo efecto

CAb pueden ser destruidos por choques repetidos

▷ **efecto de marea de la Galaxia (*tidal stripping*)**

el potencial Galáctico puede "arrancar" ☆ que alcanzan el r_t con energía suficiente

▷ **fricción dinámica**

el cúmulo pierde energía orbital para las ☆ y DM de la Galaxia

(y espirala en dirección al CG) ⇒ estímulo a evaporación y efecto de marea

▷ **difusión de estrellas de campo en el cúmulo**

captura de la ☆ → E_C transferida para el cúmulo → "calentamiento"

Tarea 6:

Investigar sobre los mecanismos de disolución presentados en esa clase.

Movimiento predominante de las estrellas e cúmulos estelares

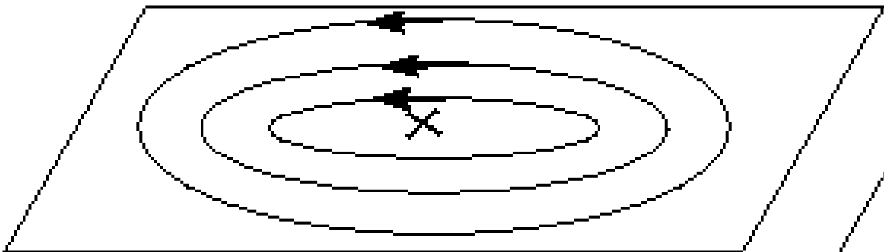

Population I stars: ordered motion.
Circular orbits in the disk plane;
younger, more metal-rich.

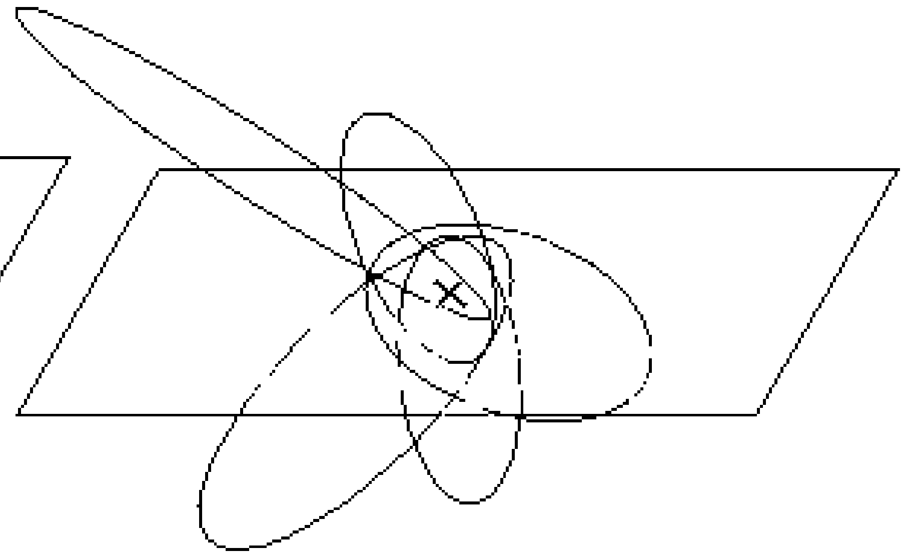

Population II stars: random motion.
Eccentric orbits passing through disk
plane; older, more metal-poor.

CAb

CGl

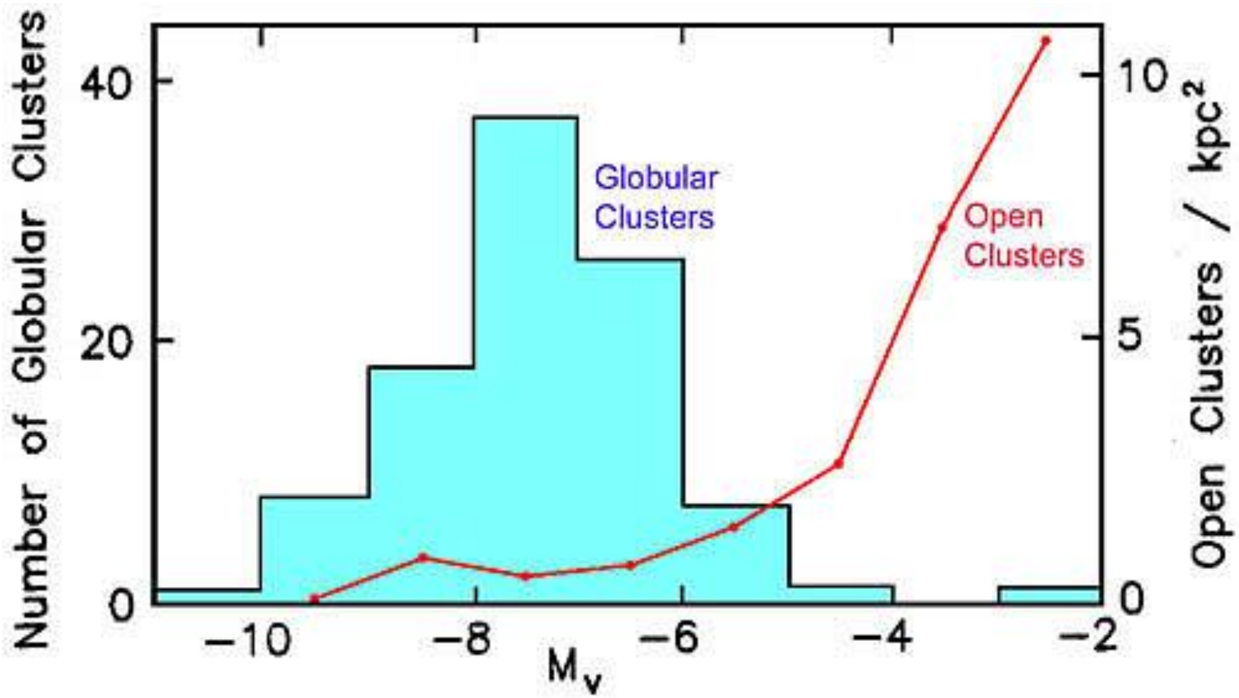
Number of Globular Clusters
Open Clusters / kpc^2
Globular Clusters
Open Clusters
M_V
40
20
0
10
5
0
−10
−8
−6
−4
−2

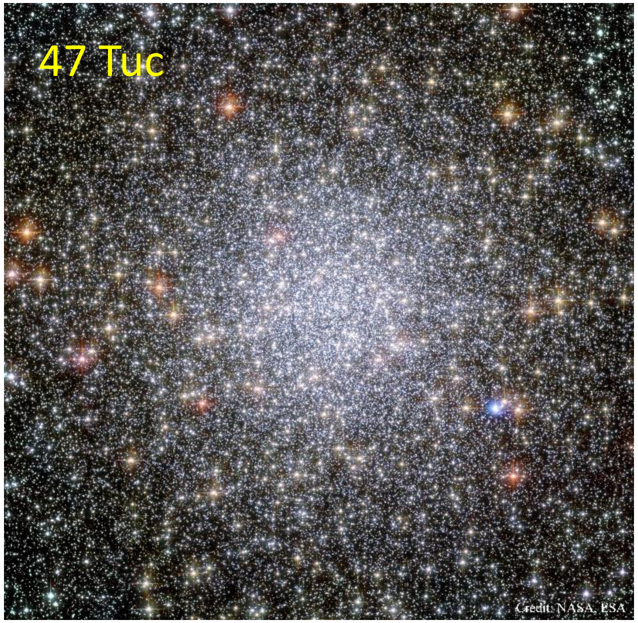
47 Tuc
Credit: NASA, ESA


M39

Subgrupos de Cúmulos Globulares

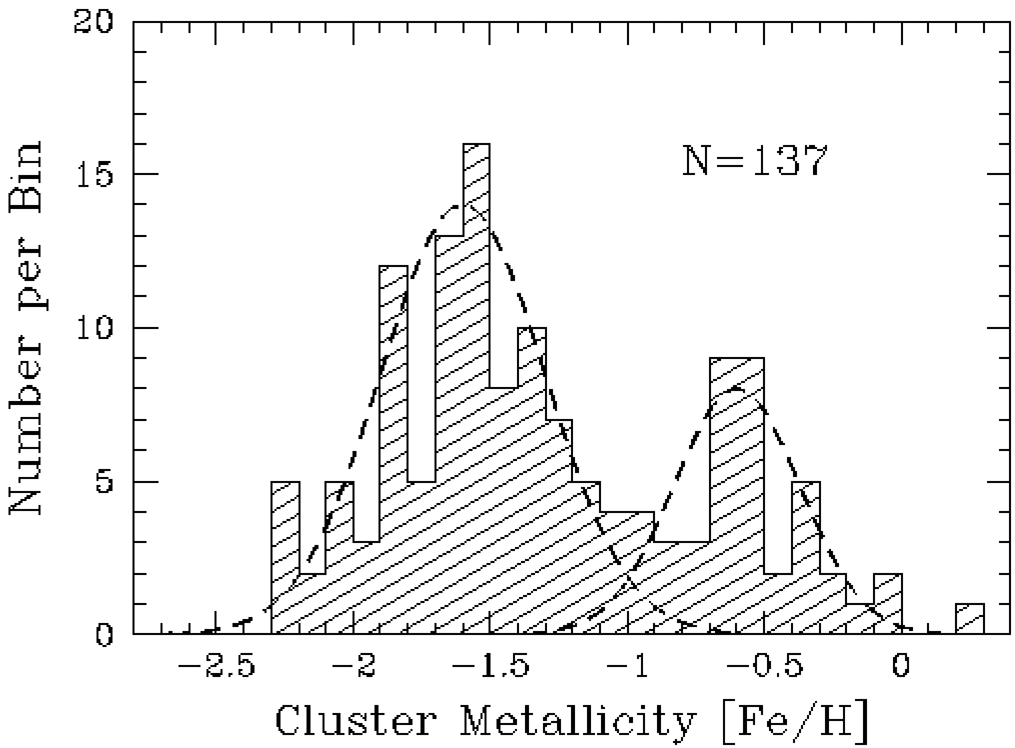

Zinn (1985), ApJ 293, 424

CPM	CRM
(clásicos del halo)	(disco grueso/bulbo)
-1.6 ± 0.30	-0.6 ± 0.23
fracción ~ 3/4	fracción ~ 1/4
distrib. esférica	R_{CG} e z pequeños

Harris (1999), Ap&SS 267, 95

Subgrupos de Cúmulos Abiertos

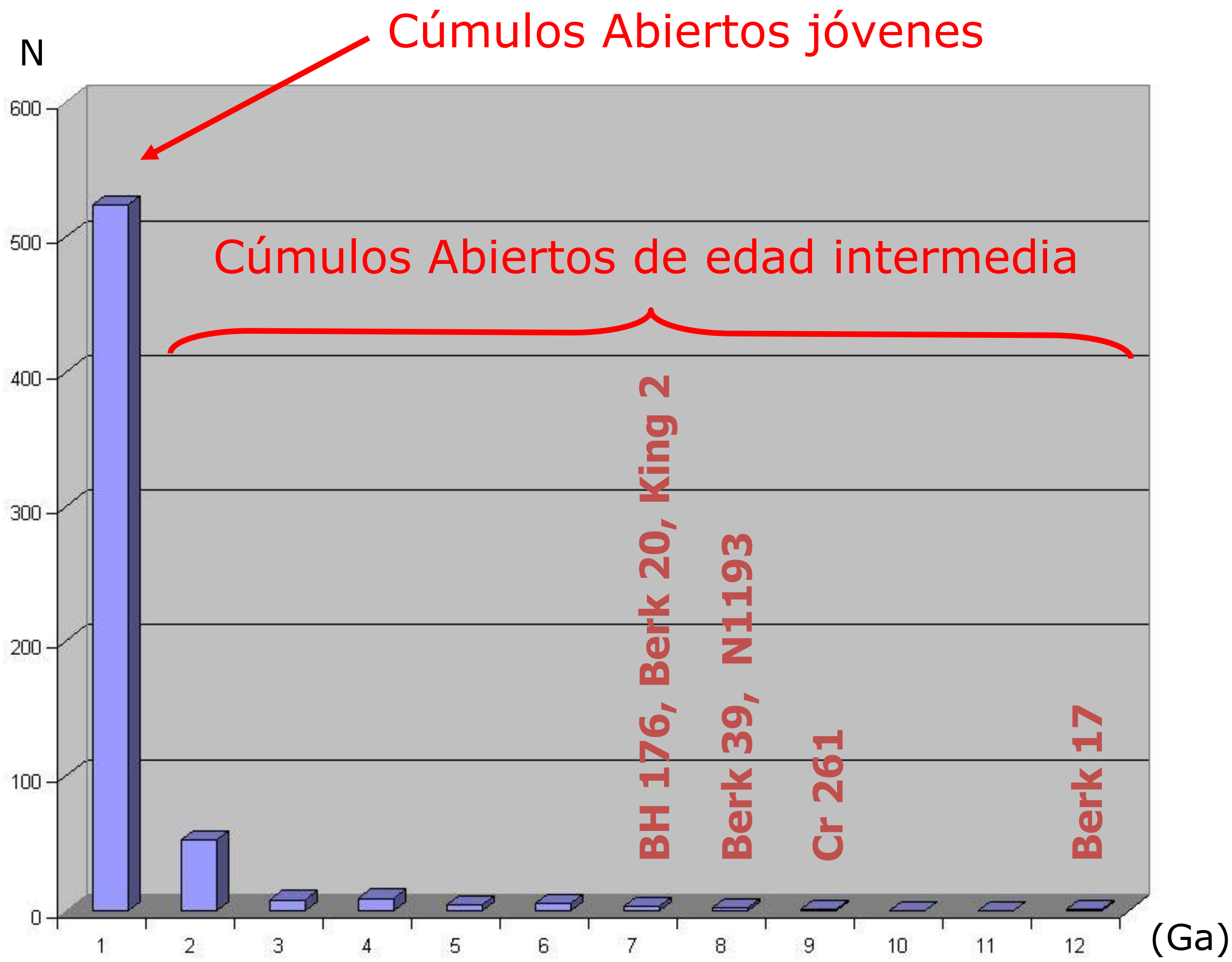

$N_{tot} = 609$

Dias et al. (2002), A&A 389, 871

Subgrupos de Cúmulos Abiertos

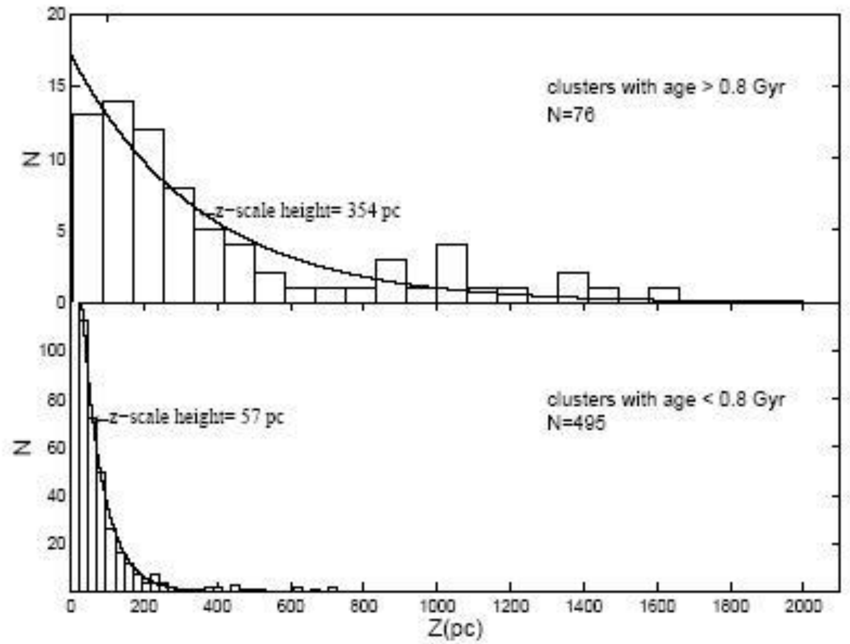

FIG. 2.—Number distribution from the Galactic plane, Z, for old and young subgroups of open clusters. The fitted scale heights for the two groups are 354 and 57 pc, respectively.

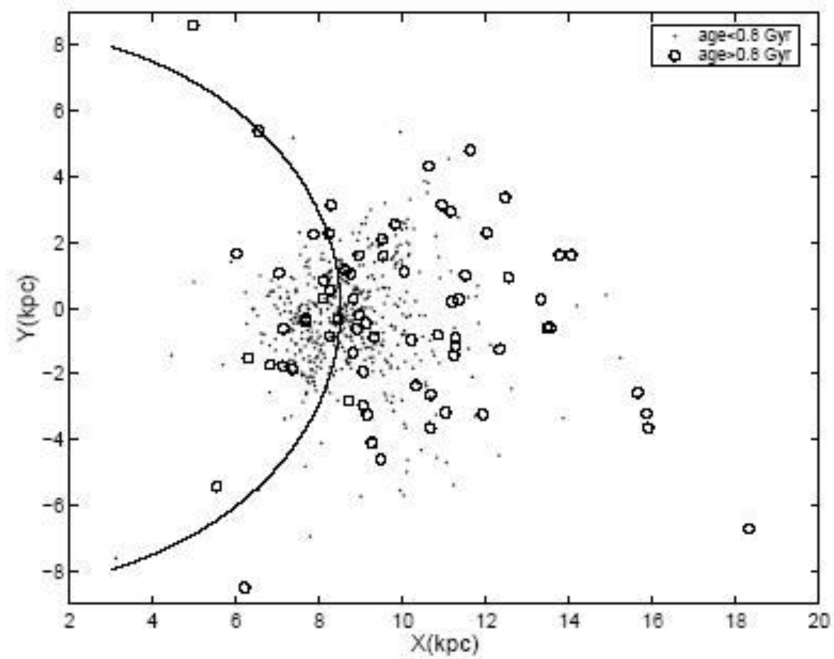

FIG. 1.—Spacial distribution of open clusters on the Galactic plane. The open circles are old clusters with ages greater than that of Hyades (0.8 Gyr), and the dots are younger ones. The Sun is at $X = 8.5$, $Y = 0$ kpc. The Galactic center is at (0, 0). The large circle has a radius of 8.5 kpc, centered on the Galactic center.

CAb viejos:

- disco grueso
- calentamiento dinámico
- acreción de satélites

Chen et al. (2003), AJ 125, 1397